Synthesis and Reactivity of Pd_2Mn, MPdFe, $MPdMn_2$, and $MPdFe_2$ Clusters (M = Pd, Pt) Stabilized by $Ph_2PCH_2PPh_2$ (dppm) Ligands. Crystal Structure of $[Pd_2Mn_2(\mu_3\text{-}CO)(\mu\text{-}CO)(CO)_7(\mu\text{-}dppm)_2]$

Pierre Braunstein,* Claude de Méric de Bellefon, and Michel Ries

Laboratoire de Chimie de Coordination, Associé au CNRS (UA 416), Université Louis Pasteur, F-67070 Strasbourg Cedex, France

Jean Fischer

Laboratoire de Cristallochimie et de Chimie Structurale, Associés au CNRS (UA 424), Université Louis Pasteur, F-67070 Strasbourg Cedex, France

Received May 22, 1987

Heterotetranuclear dppm-stabilized metalloligated clusters have been prepared by reaction of $[Fe(CO)_3NO]^-$ or $[Mn(CO)_5]^-$ with the dinuclear d^9-d^9 complexes $[PdMCl_2(\mu\text{-dppm})_2]$ (M = Pd, Pt). These clusters, of formula $[PdMFe_2(CO)_5(NO)_2(\mu\text{-dppm})_2]$ (M = Pd, **1a**; M = Pt, **1b**) and $[PdMMn_2(CO)_9(\mu\text{-dppm})_2]$ (M = Pd, **4a**; M = Pt, **4b**), are characterized by an almost planar metal core, whose Pd–M, M–Fe, and M–Mn edges are bridged by a dppm ligand. The metalloligand $Fe(CO)_3NO$ or $Mn(CO)_5$ is always connected to the triangular core PdMFe or PdMMn, respectively, via a Pd atom. This was established by an X-ray diffraction study on **4a**: monoclinic, space group $P2_1/c$, with $Z = 4$, $a = 17.561$ (7) Å, $b = 21.319$ (8) Å, $c = 19.461$ (8) Å, $\beta = 113.50$ (2)°, and d(calcd) = 1.44 g/cm^3. The structure was solved by using 4473 reflections with $I > 3\sigma(I)$ and refined to conventional $R = 0.059$ and $R_w = 0.082$. The Pd(2)–Mn(1) distance (2.580 (2) Å) is shorter than the Pd(1)–Mn(1) distance (2.698 (2) Å) and the exocyclic, unsupported Pd(1)–Mn(2) distance (2.821 (2) Å). The Pd(1)–Pd(2) distance is 2.681 (1) Å. Whereas the coordination about Mn(2) is octahedral, that about Mn(1) can be viewed as highly distorted octahedral. These clusters result from the formal insertion of a $Fe(CO)_2NO$ or $Mn(CO)_4$ fragment into the Pd–P bond of the dinuclear precursor. This accounts for the complete regioselective formation of the platinum-containing clusters in which the less labile Pt–P bonds have been retained. The chemistry reported here for the dinuclear $MPdP_4$ and for the $MPdFe_2P_4$ or $MPdMn_2P_4$ systems takes place within their plane, in contrast to the chemistry leading to A-frame structures. Furthermore, the exocyclic Pd–Fe or Pd–Mn bond of **1** or **4**, respectively, is very labile and may be broken sometimes reversibly in dissociating solvents or by other nucleophiles, e.g., halides. Whereas clusters **1** do not react with CO, $[PdMFeI(CO)_2(NO)(\mu\text{-dppm})_2]$ affords cationic clusters in the presence of $Tl[PF_6]$, which are characterized by a Pd-bound terminal CO. An effect of platinum that renders its neighboring palladium center more electron-rich is noted and influences the reactivity of the clusters. The Mn-containing clusters are generally more labile than their Fe analogues, and **4b** slowly rearranges in solution with formation of the binuclear cation $[(OC)_4Mn(\mu\text{-dppm})Pt(dppm)]^+$. All complexes were characterized by elemental analyses and IR, ^1H NMR, and $^{31}P\{^1H\}$ NMR spectroscopies. The latter is particularly informative because of the inequivalence of the four phosphorus atoms, and comparisons are made between related systems.

Introduction

As part of our research on the reactivity of carbonylmetalates toward halide complexes of the transition metals for the synthesis of mixed-metal clusters,[1] we were interested in comparing the properties of $[Co(CO)_4]^-$, $[Mn(CO)_5]^-$, and $[Fe(CO)_3(NO)]^-$ toward dinuclear d^9-d^9 Pd_2 or PdPt chloro complexes containing the $Ph_2PCH_2PPh_2$ (dppm) ligand. We have previously reported on bis dppm-bridged Pd_2Co_2 and $PdPtCo_2$ tetranuclear clusters prepared by the reaction of the cobalt tetracarbonylate anion with $[Pd_2Cl_2(\mu\text{-dppm})_2]$ or $[PdPtCl_2(\mu\text{-dppm})_2]$, respectively.[2] Studies carried out with mononuclear d^8 complexes of these metals have revealed strong differences in the nature of the products obtained depending, i.e., on the carbonylmetalates used, homo- or heteronuclear complexes of various core compositions being formed.[1,3] We wish to present here the synthesis and properties of new dppm-stabilized palladium–manganese, palladium–iron, palladium–platinum–manganese, and palladium–platinum–iron clusters. Closely related mixed Pd–Fe clusters have been found recently to be valuable precursors of new heterogeneous catalysts for the selective carbonylation of nitro derivatives.[4]

Results

Reaction of $[PdMCl_2(\mu\text{-dppm})_2]$ (M = Pd, Pt) with $K[Fe(CO)_3NO]$. The reaction of 2 mol equiv of $K[Fe(CO)_3NO]$ with $[Pd_2Cl_2(\mu\text{-dppm})_2]$ afforded the deep green mixed-metal Pd_2Fe_2 cluster **1a** in ca. 70% yield (eq 1), always accompanied by the A-frame CO-insertion product $[Pd_2Cl_2(\mu\text{-CO})(\mu\text{-dppm})_2]$ (ca. 30%).[5] The reaction was monitored by IR spectroscopy in the ν(CO) and ν(NO) regions and was stopped after stabilization of the absorption bands of the product and disappearance of the characteristic bands of $[Fe(CO)_3NO]^-$. Traces of the

(1) Braunstein, P. *Nouv. J. Chim.* **1986**, *10*, 365.
(2) (a) Braunstein, P.; Jud, J.-M.; Dusausoy, Y.; Fischer, J. *Organometallics* **1983**, *2*, 180. (b) Braunstein, P.; de Méric de Bellefon, C.; Ries, M. *J. Organomet. Chem.* **1984**, *262*, C14. (c) Braunstein, P.; de Méric de Bellefon, C.; Ries, M. *Inorg. Chem.*, in press.
(3) (a) Bender, R.; Braunstein, P.; Jud, J.-M.; Dusausoy, Y. *Inorg. Chem.* **1983**, *22*, 3394. (b) *Ibid.* **1984**, *23*, 4489. (c) Braunstein, P.; Guarino, N.; de Méric de Bellefon, C.; Richert, J.-L. *Angew. Chem., Int. Ed. Engl.* **1987**, *26*, 88.
(4) (a) Braunstein, P.; Kervennal, J.; Richert, J.-L. *Angew. Chem., Int. Ed. Engl.* **1985**, *24*, 768. (b) Braunstein, P.; Kervennal, J.; Richert, J.-L.; Ries, M. U.S. Patent 4 609 639, 1985; *Chem. Abstr.* **1986**, *104*, 19681 (to Atochem).
(5) Benner, L. S.; Balch, A. L. *J. Am. Chem. Soc.* **1978**, *100*, 6099.

0276-7333/88/2307-0332$01.50/0

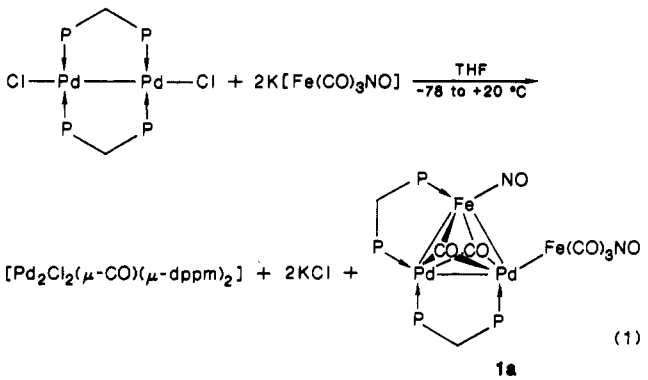

pentane-soluble complexes $[\{Fe(CO)_4\}_2(\mu\text{-dppm})]$[6a] and $[\{Fe(CO)(NO)_2\}_2(\mu\text{-dppm})]$[6b] were found in the reaction mixture. Related monophosphine-substituted iron carbonyl compounds were also formed in the reactions of mononuclear Pt or Pd phosphine complexes with $[Fe(CO)_3NO]^-$.[7] Despite numerous attempts at growing single crystals of **1a** from various solvents (THF, toluene, chlorobenzene, dichloromethane, acetone) layered with hexane (or pentane), no crystal suitable for X-ray diffraction studies was obtained. However, knowing the structure of the isoelectronic $[Pd_2Co_2(CO)_7(\mu\text{-dppm})_2]$ cluster,[2a] the structure of **1a** can be confidently deduced from spectroscopic data (see Tables I–III). Its $^{31}P\{^1H\}$ NMR spectrum exhibits a typical pattern showing three phosphorus atoms bonded to Pd centers and a fourth one bonded to a Fe atom. The coupling constants are reminiscent of those found in $[Pd_2Co_2(CO)_7(\mu\text{-dppm})_2]$, for which a detailed analysis of the spectra will be presented elsewhere. In the ^1H NMR spectrum of **1a**, the two chemically inequivalent CH_2 groups appear, respectively, as a triplet and a doublet of triplets (see below). The IR spectrum of **1a** exhibits strong carbonyl and nitrosyl stretching vibrations. By comparison with cluster **2a** where the $Fe(CO)_3NO$ fragment has been removed and replaced with I (vide infra), the highest carbonyl frequency (1978 cm^{-1}) and the lowest nitrosyl frequency (1693 cm^{-1}) are attributed to the $Fe(CO)_3NO$ metalloligand.

The formation of cluster **1a** proceeds stepwise, as evidenced by typical color changes of the reaction mixture. Starting at −78 °C with the orange color of $[Pd_2Cl_2(\mu\text{-dppm})_2]$, the solution progressively turns deep violet as the temperature is raised to ca. 0 °C. Keeping the reaction mixture at this temperature allows the persistence of the violet color for several hours. Then, increasing the temperature to ambient leads to a change of color to dark blue and then to deep green, the color of **1a**. These observations prompted us to monitor the reaction of eq 1 by variable-temperature $^{31}P\{^1H\}$ NMR spectroscopy. The spectrum of a filtered sample of the reaction mixture ($THF/CDCl_3$) at the "violet stage" (kept at −10 °C) showed two symmetrical triplets (with apparent $J(PP)$ = 35 Hz), which are reminiscent of an AA′XX′ spin system pattern. The chemical shifts values (δ −1.0 and −5.7) are in the range found for phosphorus atoms bonded to Pd(I) centers. No signal was seen in the range of chemical shifts of phosphorus atoms linked to Fe centers, and the resonance of $[Pd_2Cl_2(\mu\text{-dppm})_2]$ had completely disappeared. On the basis of these spectroscopic data, structure A is proposed

Scheme I. Proposed Intermediates in the Synthesis of 1a

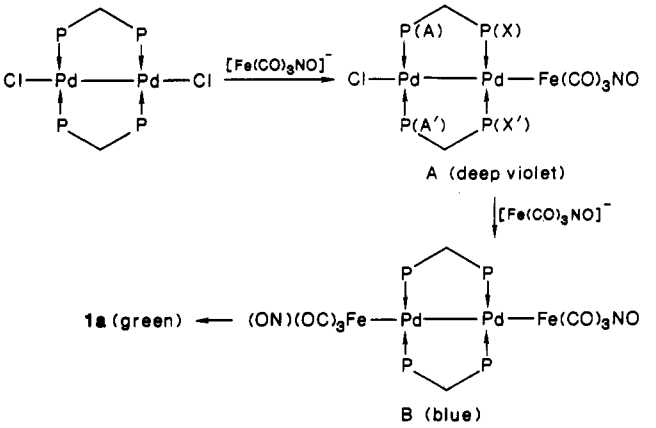

for the "violet intermediate" (Scheme I). Upon slowly raising the temperature of the sample to 0 °C, we observed the growing of a singlet at δ 0.4 and the progressive decrease of the AA′XX′ pattern. This singlet, indicating a highly symmetric species, is attributed to the intermediate B, in which the four phosphorus atoms are still bonded to Pd centers. Finally, when ambient temperature was reached, these two sets of signals disappeared, being replaced by the typical spectrum of **1a** (Table III). The growth of a signal at 11.0 ppm at this stage is attributed to an impurity resulting from slow decomposition of **1a** (see below). The violet species A was stable enough at low temperature (ca. 0 °C) to be precipitated with hexane from the reaction mixture, recovered by filtration, and washed with water to remove unreacted $K[Fe(CO)_3NO]$. The IR spectrum of the solid recorded in KBr showed two strong $\nu(CO)$ absorption bands at 1977 and 1864 cm^{-1} and a $\nu(NO)$ absorption band at 1696 cm^{-1}. These values are close to those attributed to the carbonyl and nitrosyl vibrations of the $Fe(CO)_3NO$ metalloligand in **1a** and are consistent with the structure suggested for A. It is noteworthy than when A was dissolved in THF in the absence of $K[Fe(CO)_3NO]$ and the temperature was raised to ambient, it did not afford **1a** but slowly decomposed.

Although **1a** appears stable in the solid state under N_2, its THF solutions slowly turn brown upon long standing and their $^{31}P\{^1H\}$ NMR spectra show the growing of singlets at 11.0 and −9.1 ppm. The presence of $Ph_2P(O)CH_2P(O)Ph_2$[8] is also often evidenced. On the other hand, solutions of **1a** in chlorinated solvents (e.g. $CDCl_3$, CH_2Cl_2) slowly turn red. In donor solvents such as MeCN, **1a** is partially dissociated, leading to a cationic species (eq 2).

$$[Pd_2Fe_2(CO)_5(NO)_2(\mu\text{-dppm})_2] \overset{S}{\rightleftharpoons} [Pd_2Fe(CO)_2(NO)(S)(\mu\text{-dppm})_2][Fe(CO)_3NO] \quad (2)$$
$$S = MeCN$$

The IR spectrum of an acetonitrile solution of **1a** ($\nu(CO)$ and $\nu(NO)$ absorptions) demonstrates the presence of the anion $[Fe(CO)_3NO]^-$ together with nondissociated **1a**. Evaporation of the solvent and/or addition of Et_2O causes reversal to the green color of **1a** and disappearance of the IR absorption of the anion indicates reformation of the exocyclic Pd–Fe bond.

The reaction of eq 3 affords the blue-green mixed-metal $PdPtFe_2$ cluster **1b**, analogous to **1a**. This reaction is completely *regioselective* as the only isomer observed is that in which the Pt atom is bonded to two P atoms, as clearly shown by the two large $^1J(Pt–P)$ coupling constants of 4146 and 3254 Hz in the $^{31}P\{^1H\}$ NMR spectrum of the

(6) (a) Wegner, P. A.; Evans, L. F.; Haddock, J. *Inorg. Chem.* **1975**, *14*, 192. (b) This complex will be described elsewhere,[6c] and its structure is proposed by analogy with $[Fe(CO)(NO)_2(PPh_3)]$: McBride, D. W.; Stafford, S. L.; Stone, F. G. A. *Inorg. Chem.* **1962**, *1*, 386. (c) Braunstein, P.; Richert, J.-L., to be submitted for publication.

(7) Bender, R.; Braunstein, P.; Fischer, J.; Ricard, L.; Mitschler, A. *Nouv. J. Chim.* **1981**, *5*, 81.

(8) Grim, S. O.; Walton, E. D. *Inorg. Chem.* **1980**, *19*, 1982.

$$[PdPtCl_2(\mu\text{-dppm})_2] + 2K[Fe(CO)_3NO] \xrightarrow[0-20\ ^\circ C]{THF}$$

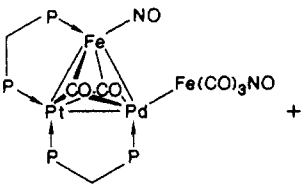

$$+ CO + 2KCl \quad (3)$$

1b

product. The other isomer, where Pd and Pt would have exchanged positions, is never observed (see Discussion). The spectroscopic data of **1b** are given in Tables I–III and are comparable with those of **1a**, with the exception of the properties associated with the presence of the Pt atom in **1b**.

Reaction of $[PdMCl_2(\mu\text{-dppm})_2]$ (M = Pd, Pt) with $Na[Mn(CO)_5]$. The reaction of $[Pd_2Cl_2(\mu\text{-dppm})_2]$ with 2 mol equiv of $Na[Mn(CO)_5]$ at low temperature gives in variable yields the tetranuclear cluster **4a** (15–25%) and the binuclear complex **6a** (10–18%) (eq 4). The manga-

$$[Pd_2Cl_2(\mu\text{-dppm})_2] + 2Na[Mn(CO)_5] \xrightarrow{THF}$$

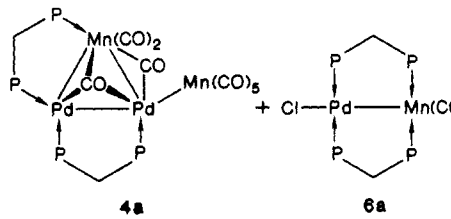

$$+ [Mn_2(CO)_{10}] + [Mn_2(CO)_8(\mu\text{-dppm})] + [Pd_2Cl_2(\mu\text{-CO})(\mu\text{-dppm})_2] + X + 2NaCl \quad (4)$$

nese complexes $[Mn_2(CO)_{10}]$ and $[Mn_2(CO)_8(\mu\text{-dppm})]$[9] are also produced, together with a small amount of the A-frame complex $[Pd_2Cl_2(\mu\text{-CO})(\mu\text{-dppm})_2]$. A third species containing Pd, Mn, and dppm (called X) is also isolated but has not been fully characterized. Isolation of the poorly stable violet cluster **4a** is best carried out following the procedure described in the Experimental Section and consisting in the total precipitation of all hexane-insoluble materials and their selective dissolution. The molecular structure of **4a** has been determined by X-ray diffraction, and ORTEP drawings are shown in Figures 1 and 2. IR and ^1H NMR data are summarized in Tables I and II, respectively. **4a** exhibits strong $\nu(CO)$ absorption bands between 2028 and 1899 cm^{-1}, attributed to linear carbonyl groups and at 1830 and 1780 cm^{-1}, for the carbonyl groups (semi) bridging the Pd(1)–Mn(1) and Pd(2)–Mn(1) bonds. The absorption at 2028 cm^{-1} clearly belongs to the $Mn(CO)_5$ group, as shown by comparison with the spectrum of $[Pd_2MnCl(CO)_4(\mu\text{-dppm})_2]$ (**5a**). Despite the low solubility of **1a**, its ^1H NMR spectrum was recorded in toluene in order to avoid the rapid decomposition that occurs in chlorinated solvents (see below). The ^1H NMR resonances of the CH_2 groups present a pattern analogous to those found for **1a**. The quality of the $^{31}P\{^1H\}$ spectra does not allow a detailed analysis (owing to ^{55}Mn quadrupole broadening and rapid decomposition), but their general pattern is consistent with that previously seen for the related $[Pd_2Co_2(CO)_7(\mu\text{-dppm})_2]$ cluster.[2a] Even stored as a solid under inert atmosphere, at low temperature, **4a** slowly decomposes after a few weeks. Its THF solutions rapidly darken, and compound X can be isolated from them. It is therefore most likely that X isolated during the synthesis of **4a** originates from the degradation of the

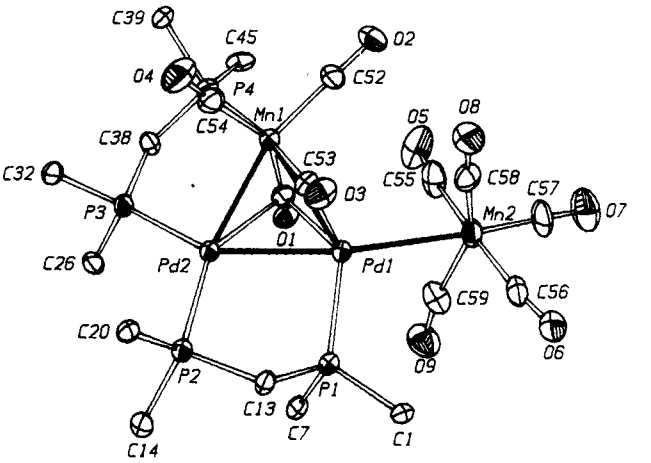

Figure 1. Molecular structure of $[Pd_2Mn_2(\mu_3\text{-CO})(\mu\text{-CO})(CO)_7(\mu\text{-dppm})_2]$ (**4a**) top view) illustrating the atom numbering scheme. For clarity, the eight phenyl groups are represented by their ipso carbon atoms only. Thermal ellipsoids enclose 50% of the electron density.

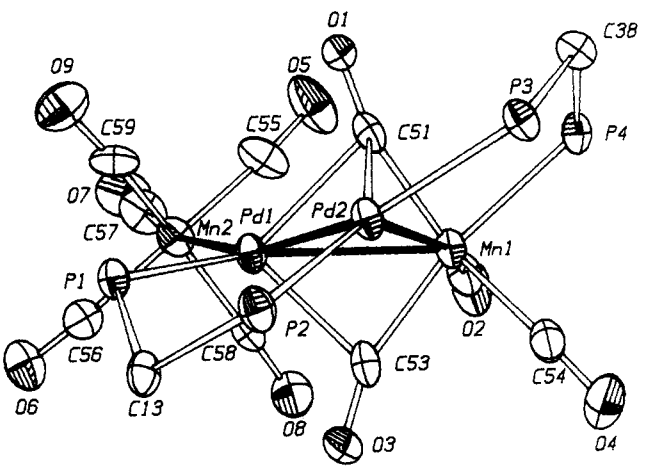

Figure 2. Perspective drawing of the molecular structure of $[Pd_2Mn_2(\mu_3\text{-CO})(\mu\text{-CO})(CO)_7(\mu\text{-dppm})_2]$ (**4a**). Phenyl groups omitted for clarity.

latter in solution. When the reaction of eq 4 was carried out at ambient temperature, neither **4a** nor **6a** were isolated but X was recovered as the only Pd, Mn-containing species. It presents two strong $\nu(CO)$ absorption bands in the IR, and its ^1H NMR spectrum exhibits a broad and unresolved multiplet at δ 3.73 assigned to the methylene resonance of the dppm ligand. $^{31}P\{^1H\}$ NMR spectra are hardly recordable (apparent paramagnetism due to X or to remaining impurities, despite numerous purification steps by column chromatography). In order to chemically characterize X, we reacted it with various nucleophiles, but no reaction occurred with I^-, $[Mn(CO)_5]^-$, CO (in THF), or phosphines (PPh_3, dppm in CH_2Cl_2).

We have independently checked that the complex $[PdMnCl(CO)_3(\mu\text{-dppm})_2]$ (**6a**)[10] does not result from the reaction of NaCl with **4a** nor is it formed via a cationic species such as $[Pd_2Mn(CO)_4(\mu\text{-dppm})_2(solv)]^+$, which could be a precursor of stable **5a**. However, we cannot rule out a reaction involving other degradation products of **4a** as contributing to the formation of **6a**. Since our preliminary publication describing the formation of **6a** in the reaction of $[PdCl_2(PhCN)_2]$ with $[Mn(CO)_5]^-$ and dppm,[10] a higher yield synthesis of **6a** has been reported, starting from a Pd(0) complex and $[Mn(CO)_5Cl]$.[11b,c]

(9) (a) Reimann, R. H.; Singleton, E. *J. Organomet. Chem.* **1972**, *38*, 113. (b) Colton, R.; Commons, C. J. *Aust. J. Chem.* **1975**, *28*, 1673.

(10) Braunstein, P.; Jud, J.-M.; Fischer, J. *J. Chem. Soc., Chem. Commun.* **1983**, 5.

Table I. Infrared Spectral Data

complex	IR abs max ν(CO),[a] cm^{-1}		IR abs max ν(NO),[a] cm^{-1}	
	solid state (KBr)	solution (THF)	solid state (KBr)	solution (THF)
$[Pd_2Fe_2(CO)_5(NO)_2(\mu\text{-dppm})_2]$ (**1a**)	1974 (s), 1875 (s, br), 1840 (sh)	1978 (s), 1902 (sh), 1876 (s), 1843 (w)	1737 (s), 1683 (s)	1757 (sh), 1742 (s), 1693 (s)
$[PdPtFe_2(CO)_5(NO)_2(\mu\text{-dppm})_2]$ (**1b**)	1969 (s), 1905 (sh), 1882 (vs br), 1834 (sh)	1973 (s), 1891 (s), 1876 (s)	1741 (s), 1672 (s)	1759 (sh), 1749 (s), 1688 (s)
$[Pd_2FeI(CO)_2(NO)(\mu\text{-dppm})_2]$ (**2a**)	1875 (w sh), 1828 (s)	1872 (w), 1830 (s)	1736 (s)	1746 (s)
$[PdPtFeI(CO)_2(NO)(\mu\text{-dppm})_2]$ (**2b**)	1879 (w sh), 1826 (s, br)	1876 (w, br), 1829 (m)	1734 (vs br)	1751 (s)
$[Pd_2FeCl(CO)_2(NO)(\mu\text{-dppm})_2]$	1884 (w sh), 1834 (s, br)		1741 (vs br)	
$[Pd_2Fe(CO)_3(NO)(\mu\text{-dppm})_2][PF_6]$ (**3a**)[b]	2065 (s), 1862 (s)	2069 (s), 1869 (s)	1743 (vs)	1757 (vs)
$[PdPtFe(CO)_3(NO)(\mu\text{-dppm})_2][PF_6]$ (**3b**)[b]	2063 (s), 1857 (s, br)	2067 (s), 1863 (s, br)	1749 (vs)	1756 (vs)
$[Pd_2Mn_2(CO)_9(\mu\text{-dppm})_2]$ (**4a**)	2028 (vs), 1973 (s), 1927 (vs), 1899 (vs), 1830 (w, br), 1780 (w, br)			
$[PdPtMn_2(CO)_9(\mu\text{-dppm})_2]$ (**4b**)	2028 (s), 1971 (s), 1903 (s, br)			
$[Pd_2MnCl(CO)_4(\mu\text{-dppm})_2]$ (**5a**)[c]	1978 (vs), 1916 (vs), 1840 (w, br), 1780 (w, br)	1982 (vs), 1925 (s)		

[a] Abbreviations: vs, very strong; s, strong; m, medium; sh, shoulder; br, broad; w, weak. [b] For PF_6^-, the ν(PF) value recorded in KBr is 840 (vs) cm^{-1}. [c] Values recorded as mineral oil mull: 1980 (vs), 1916 (s) cm^{-1}.

Table II. ^1H NMR Data[a]

complex	P–CH_2–P[b]				P–CH_2–P[b]		
	δ	^2J(P–H), Hz	^4J(P–H), Hz	^3J(Pt–H), Hz	δ	^2J(P–H), Hz	^3J(Pt–H), Hz
$[Pd_2Fe_2(CO)_5(NO)_2(\mu\text{-dppm})_2]$ (**1a**)	4.50 (dt)	8.4	2.5		3.91 (t)	9.8	
$[PdPtFe_2(CO)_5(NO)_2(\mu\text{-dppm})_2]$ (**1b**)	4.87 (t)	9.0		71	4.18 (t)	10.0	33
$[Pd_2FeI(CO)_2(NO)(\mu\text{-dppm})_2]$ (**2a**)	4.51 (t)	8.3			4.09 (t)	9.5	
$[Pd_2FeCl(CO)_2(NO)(\mu\text{-dppm})_2]$	4.27 (dt)	8.3	3.0		3.96 (t)	9.8	
$[PdPtFeI(CO)_2(NO)(\mu\text{-dppm})_2]$ (**2b**)	4.81 (dd)	11.5	5.5	56	4.41 (t)	8.4	37
$[Pd_2Fe(CO)_3(NO)(\mu\text{-dppm})_2][PF_6]$ (**3a**)	4.65 (dt)	10.0	2.4		4.32 (t)	10.4	
$[Pd_2Mn_2(CO)_9(\mu\text{-dppm})_2]$ (**4a**)[c]	4.45 (dt)	8.5	3.6		4.05 (t)	9.7	
$[Pd_2MnCl(CO)_4(\mu\text{-dppm})_2]$ (**5a**)	4.35 (t)	10.4			3.98 (t)	8.7	

[a] In $CDCl_3$. Abbreviations: t, triplet; dt, doublet of triplet; dd, doublet of doublet. All compounds exhibit complex multiplets due to the phenyl groups of the dppm ligands in the range 7.5–6.8 ppm (40 H). [b] The integration of the P–CH_2–P resonances corresponds to 2 H. [c] Recorded in toluene-d_8.

Table III. $^{31}P\{^1H\}$ NMR Data[a]

complex	δ[b]				|J(P–P)|, Hz						|J(Pt–P)|, Hz			
	δ_4	δ_3	δ_2	δ_1	P^1P^2	P^1P^3	P^1P^4	P^2P^3	P^2P^4	P^3P^4	PtP^1	PtP^2	PtP^3	PtP^4
$[Pd_2Fe_2(CO)_5(NO)_2(\mu\text{-dppm})_2]$ (**1a**)	41.95	4.35	−4.14	1.86	90	22	93	51	56	23				
$[PdPtFe_2(CO)_5(NO)_2(\mu\text{-dppm})_2]$ (**1b**)	37.08	13.15	6.01	3.10	90	16	92	7	45	18	*c*	3254	4146	*c*
$[Pd_2FeI(CO)_2(NO)(\mu\text{-dppm})_2]$ (**2a**)	38.51	0.02	−14.72	−0.18	77	11	83	51	53	22				
$[PdPtFeI(CO)_2(NO)(\mu\text{-dppm})_2]$ (**2b**)[d]	35.16	10.55	−0.37	−1.51	74	14.5	88	6.5	48	15	57	3327.5	4035	59
$[Pd_2Fe(CO)_3(\mu\text{-dppm})_2][PF_6]$ (**3a**)[e]	34.72	−0.85	−10.20	−2.58	48	≤5	61	45	34	15				
$[PdPtFe(CO)_3(NO)(\mu\text{-dppm})_2][PF_6]$ (**3b**)[e]	30.08	7.45	0.91	−4.57	53	13.5	65	14	31.5	13	55	3140	3941	45
$[Pd_2MnCl(CO)_4(\mu\text{-dppm})_2]$ (**5a**)[f]	64.12	−1.36	11.63	2.91	64	21	57	72	7	20				

[a] In $CH_2Cl_2/CDCl_3$ (1:1). [b] For phosphorus labeling, see Chart I. [c] Poor resolution prevents a detailed analysis. [d] In THF/C_6D_6 (2:1). [e] Recorded under CO atmosphere, the $[PF_6]^-$ anion exhibits a septuplet at −143.9 ppm (^1J(PF) = 709 Hz). [f] For phosphorus assignment, see Discussion.

The reaction of $[PdPtCl_2(\mu\text{-dppm})_2]$ with 2 mol equiv of $Na[Mn(CO)_5]$ in THF at low to room temperature affords the green-brown tetranuclear cluster **4b** in moderate yield (eq 5). Despite the relative instability of **4b**, its structure is confidently proposed by comparison of its spectroscopic data with those of **4a**. As for the other members of the metalloligated $PdPtM_2(\mu\text{-dppm})_2$ family,[2] only the isomer in which the Pd atom is bonded to the two M atoms was evidenced. It is noteworthy that in contrast to the reaction of eq 4, that of eq 5 did not produce a heterobinuclear complex analogous to **6a** nor afford dppm-substituted manganese carbonyl species. Cluster **4b** in solution easily transforms into new species among which the cation $[(OC)_4Mn(\mu\text{-dppm})Pt(dppm)]^+$ (**7b**) could be identified by $^{31}P\{^1H\}$ NMR spectroscopy and comparison with an authentic sample. Thus, cation **7b** has been

$$[PdPtCl_2(\mu\text{-dppm})_2] + 2Na[Mn(CO)_5] \xrightarrow{THF}$$

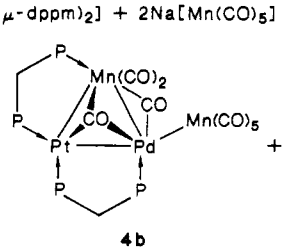

4b

$$+ [Mn_2(CO)_{10}] + 2NaCl \quad (5)$$

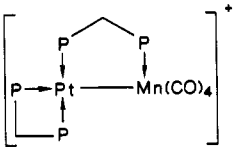

7b

(11) (a) Braunstein, P.; Jud, J.-M.; Fischer, J., unpublished results, 1982. (b) Hoskins, B. F.; Steen, R. J.; Turney, T. W. *Inorg. Chim. Acta* **1983**, *77*, L69. (c) *J. Chem. Soc., Dalton Trans.* **1984**, 1831.

prepared independently by the reaction of *trans*-[Pt{Mn(CO)$_5$}$_2$(PhCN)$_2$] with two equiv of dppm.[12]

Preparation and Characterization of [PdMFeI(CO)$_2$(NO)(μ-dppm)$_2$] (M = Pd, 2a; M = Pt, 2b) and [Pd$_2$MnCl(CO)$_4$(μ-dppm)$_2$] (5a). The reaction of **1a** with iodide in acetone is instantaneous and affords in high yield the trinuclear cluster [Pd$_2$FeI(CO)$_2$(NO)(μ-dppm)$_2$] (**2a**) which can be isolated in the solid state, according to the procedure described in the Experimental Section where addition of water plays a critical role. In the absence of

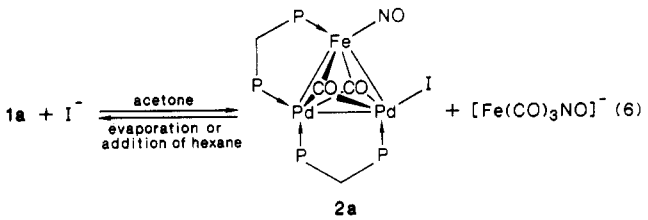

2a

water, the equilibrium of eq 6 is easily reversed either by adding a nonsolvent (hexane, pentane) or by evaporating the reaction mixture to dryness, indicating that precipitation of **1a** is preferred over that of **2a**, even in the presence of a large excess of I$^-$. A similar equilibrium was also observed in the reaction of [Pd$_2$Co$_2$(CO)$_7$(μ-dppm)$_2$] with halides.[2b]

The related PdPtFe$_2$ cluster **1b** also reacts with KI, affording **2b**. Interestingly, it is possible to isolate **2b**

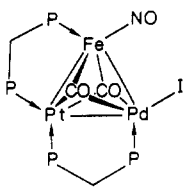

2b

simply by solvent evaporation because it does not react with the [Fe(CO)$_3$NO]$^-$ present. This contrasts with the behavior of **2a** which gives **1a** under similar conditions. Clusters **2** were characterized by their ^{1}H and ^{31}P{^{1}H} NMR data which are closely related to those of **1** (Tables II and III). In particular, no isomerization of the FePdPtP$_4$ core is observed during the reactions of **1b** or **2b**. Infrared data for these clusters are given in Table I.

When the Pd$_2$Mn$_2$ cluster **4a** is treated with nonfreshly distilled CH$_2$Cl$_2$, it undergoes a clean reaction leading to green **5a**. By contrast with **4a**, **5a** appears to be very stable

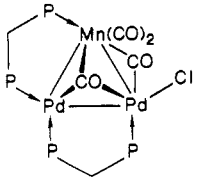

5a

and detailed spectroscopic investigations could be carried out. The ^{31}P{^{1}H} spectrum shows well-resolved signals corresponding to a manganese-bound P atom and three palladium-bound P atoms and presents a general pattern typical for the Pd$_2$M(μ-dppm)$_2$ family (Table III). The ^{1}H NMR spectrum shows that the two groups of signals due to the methylene protons are shifted upfield with respect to those of **4a** (Table II). The IR spectrum exhibits only two strong ν(CO) bands. The highest frequency band due to the carbonyls of the exocyclic Mn(CO)$_5$ fragment of **4a** has completely disappeared (Table I). These data are consistent with the formulation [Pd$_2$MnCl(CO)$_4$(μ-dppm)$_2$] and the structure shown which derives from **4a** by substitution of the exocyclic Mn(CO)$_5$ fragment by Cl. The mechanism of the reaction leading to **5a** is not yet clearly elucidated. In order to check the origin of the chloride in **5a**, we treated **4a** with carefully distilled CH$_2$Cl$_2$ and no reaction occurred. On the other hand, the reaction of **4a** with commercial-grade CDCl$_3$ or "old" CHCl$_3$ led to immediate formation of **5a**. Reactions of **4a** with freshly distilled CH$_2$Cl$_2$ containing a small amount of NaCl or HCl were also carried out. No immediate reaction occurred, ruling out rapid attack of Cl$^-$ on **4a**. All these observations lead us to consider a radical process involving Cl$^\bullet$ attack on the Pd(1)–Mn(2) bond as the most probable. It is well-known that Cl$^\bullet$ radicals may be generated by decomposition of chlorinated solvents. However, the synthesis of **5a** can be achieved in ca. 80% yield by treating **4a** with HCl. Some decomposition occurs, and no byproduct could be identified, although [HMn(CO)$_5$] is most likely formed in this reaction. Electrophilic assistance by H$^+$ is thus beneficial for the transformation **4a** → **5a** as the latter does not react with NaCl in THF, probably also owing to the low solubility of NaCl in this medium. However, the reaction of **4a** with chloride ions can be performed by adding a few drops of water to the solvent or working with more soluble chloride salts, such as [NEt$_4$]Cl or [PPN]Cl. But even with an excess of such halides, the reaction is never complete and a complex mixture of **4a**, **5a**, X, and *fac*-[MnCl(CO)$_3$(dppm)] is formed[13] (the latter was not seen in the reaction with HCl). The formation of **5a** proceeds by displacement of the equilibrium of eq 7, but rapid

$$\mathbf{4a} + Cl^- \rightleftharpoons \mathbf{5a} + [Mn(CO)_5]^- \qquad (7)$$

decomposition of unstable **4a** occurs simultaneously. However, shifting the equilibrium of eq 7 to the left can be achieved by adding a nonsolvent, such as hexane, to the reaction mixture. This should be done at a very early stage of the reaction, before decomposition begins.

Reactions of 2a, 2b, and 5a with CO. The reaction of **2a** or **2b** with CO in the presence of a stoichiometric amount of, e.g., Tl[PF$_6$] leads to the quantitative formation of the cationic cluster **3a** or **3b** (Scheme II). Clusters **3a** and **3b** exhibit a new strong ν(CO) absorption band in THF at 2069 and 2067 cm^{-1}, respectively, which is consistent with a carbonyl ligand terminally bound to the Pd atom. The other carbonyl and nitrosyl frequencies are shifted to higher wavenumbers in comparison with those in **2**, in accord with **3** being cationic species. The presence of [PF$_6$]$^-$ is evidenced by IR and ^{31}P{^{1}H} NMR spectroscopy. In the absence of an halide abstractor, no reaction occurred in THF between **1a**, **2a**, or **2b** and CO. These clusters therefore appear more stable toward CO than [Pd$_2$Fe(CO)$_4$(μ-dppm)$_2$][4a] or than **5a** which decompose under these conditions, with formation in the latter case of, e.g., *fac*-[MnCl(CO)$_3$(dppm)], a complex also observed when **4a** is reacted with chloride ions.

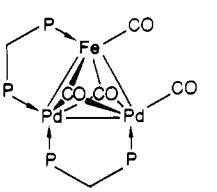

(12) De Méric de Bellefon, C. Thèse de Spécialité, Université Louis Pasteur, Strasbourg, 1985, Chapter III.

(13) Colton, R.; McCormick, M. J. *Aust. J. Chem.* **1976**, *29*, 1657.

Scheme II

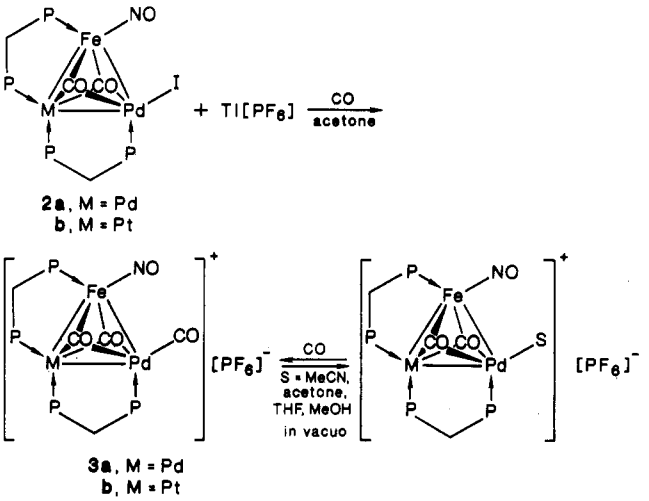

The palladium-bound carbonyl ligand in **3** is almost quantitatively removed by evaporation of the solvent under reduced pressure (Scheme II). Bubbling CO through the solution regenerates **3**. This reversible CO uptake can be monitored by IR spectroscopy, following the change of intensity of the ν(CO) vibration band at 2069 or 2067 cm^{-1}, respectively. As expected, the cationic clusters **3** are very reactive toward nucleophiles. Thus for example, reaction of **3a** with NaCl in solution affords the neutral trinuclear cluster $[Pd_2FeCl(CO)_2(NO)(\mu\text{-dppm})_2]$.[2c] However, the IR spectrum of **3a** can be recorded in KBr pellets without a solid-state reaction with Br^- and loss of CO occurring, as indicated by unchanged ν(CO) frequencies. **3b** was reacted with NaOCHO, with the hope of forming a hydrido trimetallic cluster. A dark blue-green complex formed for which, however, no detailed structure can be proposed at the present time, except that the triangulo $(\mu\text{-dppm})_2$ core is maintained.

X-ray Diffraction Study of $[Pd_2Mn_2(\mu_3\text{-CO})(\mu\text{-CO})(CO)_7(\mu\text{-dppm})_2]\cdot C_6H_5Cl$ (4a). ORTEP drawings of **4a** (top and side views) are shown in Figures 1 and 2. Selected bond distances and angles are given in Table IV. There are no short contacts between the cluster and the chlorobenzene molecule of solvation. The framework of this heterotetranuclear metalloligated cluster consists of a triangulo Pd(1)–Pd(2)–Mn(1) unit, of which the edges Pd(1)–Pd(2) and Pd(2)–Mn(1) are spanned by a dppm ligand, and of a $Mn(CO)_5$ group connected to it via Pd(1). This unusual structure is however comparable to that of the tetranuclear cluster $[Pd_2Co_2(CO)_7(\mu\text{-dppm})_2]$.[2a] The Pd(1)–Pd(2) distance in **4a** [2.681 (1) Å] falls in the range of Pd–Pd bonds bridged by one or two dppm ligands.[3a] The Pd(2)–Mn(1) distance [2.580 (2) Å] is much shorter than the Pd–Mn distance in the binuclear complexes $[PdMnX(CO)_3(\mu\text{-dppm})_2]$ [X = Cl, 2.814 Å;[11a] X = Br, 2.810 (2) Å[11b,c]] or than the two other Pd–Mn bonds in **4a**, the longest being the exocyclic Pd(1)–Mn(2) bond. These distances were the first ones to have been reported for palladium–manganese bonds.[10] The four metallic atoms are almost coplanar, Mn(2) lying slightly out of the triangular plane. This deviation (0.715 Å) is more important than the corresponding one in $[Pd_2Co_2(CO)_7(\mu\text{-dppm})_2]$.[2a] Deviations from coplanarity are also seen for the phosphorus atoms of the dppm ligands, and P(1) and P(2) lie above the triangular plane whereas P(3) and P(4) lie under this plane. The maximum deviation occurs for P(4) [1.438 (4) Å]. On the other hand, the P(1)Pd(1)Pd(2) angle [83.21 (8)°] is smaller than the corresponding angles in, e.g., $[Pd_2Br_2(\mu\text{-dppm})_2]$[14] or $[Pd_2Co_2(CO)_7(\mu\text{-dppm})_2]$,[2a] and this results from an increased steric constraint due to the exocyclic $Mn(CO)_5$ fragment, compared to the smaller Br or $Co(CO)_4$ groups. The coordination about Mn(2) is octahedral. The five carbonyl groups borne by Mn(2) are linear, and no significant interaction with the neighboring Pd(1) center is evidenced. The average Mn(2)–C distances are normal. Of the four carbonyl groups borne by Mn(1), only C(52)O(2) and C(54)O(4) are truly terminal. When considering the Pd(1)C(53) distance of 2.14 (1) Å and the Mn(1)C(53)O(3) angle of 159(1)°, the carbonyl ligand C(53)O(3) can be considered as semibridging the Pd(1)–Mn(1) bond. Similar considerations lead to view C(51)O(1) as capping the metallic triangle in a semi triply bridging fashion. The coordination about Mn(1) may be viewed as highly distorded octahedral with the C(51), C(53), Pd(2) face being capped by the Pd(1) atom (Figure 2).

Table IV. Selected Interatomic Distances and Angles in $4a\cdot C_6H_5Cl$[a,b]

Bond Lengths (Å)			
Pd(1)–Pd(2)	2.681 (1)	Pd(1)–C(51)	2.28 (1)
Pd(1)–Mn(1)	2.698 (2)	Pd(1)–C(53)	2.14 (1)
Pd(1)–Mn(2)	2.821 (2)	Pd(2)–C(51)	2.43 (2)
Pd(2)–Mn(1)	2.580 (2)	Pd(2)–C(53)	2.82 (1)
Pd(1)–P(1)	2.324 (4)	Mn(2)–C(55)	1.80 (2)
Pd(2)–P(2)	2.360 (4)	Mn(2)–C(56)	1.85 (2)
Pd(2)–P(3)	2.273 (3)	Mn(2)–C(57)	1.74 (2)
Mn(1)–P(4)	2.292 (4)	Mn(2)–C(58)	1.81 (1)
Mn(1)–C(51)	1.92 (1)	Mn(2)–C(59)	1.77 (1)
Mn(1)–C(52)	1.80 (1)	C(51)–O(1)	1.16 (1)
Mn(1)–C(53)	1.94 (2)	C(53)–O(3)	1.14 (1)
Mn(1)–C(54)	1.86 (1)		

Bond Angles (deg)			
Pd(2)–Pd(1)–Mn(1)	57.33 (4)	C(53)–Mn(1)–C(54)	80.3 (6)
Pd(2)–Pd(1)–Mn(2)	163.39 (7)	C(55)–Mn(2)–C(58)	94.4 (7)
Mn(1)–Pd(1)–Mn(2)	113.96 (7)	C(56)–Mn(2)–C(58)	85.9 (6)
Pd(1)–Pd(2)–Mn(1)	61.67 (5)	C(56)–Mn(2)–C(59)	89.6 (7)
Pd(2)–Pd(1)–P(1)	83.21 (8)	C(55)–Mn(2)–C(57)	88.0 (8)
Pd(1)–Pd(2)–P(2)	101.20 (8)	Mn(1)–C(51)–O(1)	164 (1)
Mn(1)–Pd(2)–P(3)	91.1 (1)	Mn(1)–C(53)–O(3)	159 (1)
P(2)–Pd(2)–P(3)	113.9 (1)	Mn(2)–C(55)–O(5)	172 (1)
Pd(2)–Mn(1)–P(4)	99.5 (1)	Mn(2)–C(56)–O(6)	171 (1)
P(4)–Mn(1)–C(51)	82.2 (4)	Mn(2)–C(57)–O(7)	178 (1)
C(51)–Mn(1)–C(52)	110.3 (6)	Mn(2)–C(58)–O(8)	176 (1)
C(52)–Mn(1)–C(53)	92.4 (6)	Mn(2)–C(59)–O(9)	169 (1)

[a] Atoms are labeled in agreement with Figures 1 and 2. [b] Numbers in parentheses are estimated standard deviations in the last significant digit.

Discussion

Synthesis and Reactivity. The reaction of carbonylmetalate anions with binuclear Pd–Pd or Pd–Pt complexes has been shown to lead to new heterotetranuclear clusters. This reaction is fast and, in the case of the Pd–Pd systems, must be started at low temperature, consistent with the enhanced reactivity of palladium vs platinum complexes. The reaction of $[Fe(CO)_3NO]^-$ with $[Pd_2Cl_2(\mu\text{-dppm})_2]$ or $[PdPtCl_2(\mu\text{-dppm})_2]$ compares well with the reactions previously carried out with the isoelectronic anion $[Co(CO)_4]^-$, and the general properties of the resulting clusters are very similar. A spectroscopic study of the intermediate species formed during this reaction has allowed us to reasonably assume that the first step is the replacement of a chloride by the carbonylmetalate anion, the resulting linear trimetallic complex being relatively stable at low temperature. The following step would be the replacement of the second chloride by the carbonylmetalate anion, leading to a very unstable linear tetranu-

(14) Holloway, R. G.; Penfold, B. R.; Colton, R.; McCormick, M. J. *J. Chem. Soc., Chem. Commun.* **1976**, 485.

clear complex that immediately rearranges into the final product. This occurs via P–Pd bond breaking, formation of a P–Fe bond, and loss of a CO ligand. The greater lability of the P–Pd vs the P–Pt bond explains the completely selective formation of only one isomer in these reactions. It is noteworthy that the binuclear A-frame complex $[Pd_2Cl_2(\mu\text{-}CO)(\mu\text{-}dppm)_2]$[5] is always formed when starting from $[Pd_2Cl_2(\mu\text{-}dppm)_2]$, as the latter is easily carbonylated by the CO liberated during the synthesis of **4a**. This is consistent with the absence in the reactions of eq 3 and 5 of $[PdPtCl_2(\mu\text{-}CO)(\mu\text{-}dppm)_2]$, which is not as easily made by carbonylation of $[PdPtCl_2(\mu\text{-}dppm)_2]$.[15] We have independently shown that $[Pd_2Cl_2(\mu\text{-}CO)(\mu\text{-}dppm)_2]$ does not react with carbonylmetalates under mild conditions and is therefore not a reaction intermediate.

The reactivity of these Pd_2Fe and PdPtFe clusters is very similar to that of analogous systems where Fe(NO) is replaced by Co(CO). The more labile bond is always the exocyclic Pd–Fe bond. It is reversibly broken by dissociating solvents or by anionic nucleophiles such as iodide (depending on the solvent). Cationic clusters $[PdMFe(CO)_3(NO)(\mu\text{-}dppm)_2]^+$ (M = Pd, Pt) were obtained by the clean reaction of neutral trinuclear iodo precursors **2a** and **2b** with $Tl[PF_6]$ under CO. The coordination of the carbonyl ligand on Pd is reversible under mild conditions. When going from **1a**, **2a**, or **3a** to **1b**, **2b**, or **3b**, respectively, the reactivity of the clusters is modified along the same trends as noted in the corresponding cobalt-containing clusters. The presence of platinum in these clusters renders its neighboring palladium center more electron-rich and therefore influences its reactivity toward, e.g., nucleophiles. Such an effect has been noted in related systems and will not be detailed here.[2c]

The reactions of the Pd–Pd or Pd–Pt precursors with $[Mn(CO)_5]^-$ give rise to more products than those with the $[Co(CO)_4]^-$ or $[Fe(CO)_3NO]^-$ anions, and no intermediate could be clearly identified. Such differences could be accounted for by the relative stabilities of the intermediates, which can evolve via various reaction pathways, leading to, e.g., clusters **4**, the bimetallic **6a**, $[Mn_2(CO)_{10}]$, and $[Mn_2(CO)_8(\mu\text{-}dppm)]$. The Pd_2Mn_2 cluster **4a** is less stable as a solid and in solution than **1a** or $[Pd_2Co_2(CO)_7(\mu\text{-}dppm)_2]$. This results from a very labile exocyclic Pd(1)–Mn(2) bond, the most reactive site of **4a**, and from a triangulo Pd_2Mn core being also more reactive than its Pd_2Fe or Pd_2Co analogues. The reaction of **4a** with CH_2Cl_2 or $CDCl_3$, leading to **5a**, is not well-understood, but related reactions between chlorinated solvents and metal–metal bonds (especially involving Mn group metals) have been previously reported.[16] Reaction of **4a** with Cl^- leads to **5a** and decomposition products, but **6a** is not formed, indicating that the latter is produced during the synthesis of **4a** by an independent pathway. In contrast, **4b** slowly rearranges in solution with formation of the binuclear cation $[(OC)_4Mn(\mu\text{-}dppm)\ Pt(dppm)]^+$ (**7b**).[12] Even the trinuclear core of **5a** is broken by mild reagents such as CO, and a mononuclear Mn fragment is expelled from the cluster. Such an instability probably results from both electronic and steric effects, induced by the presence of manganese–carbonyl fragments in the molecule. These are reflected by the strong influence of Mn on the chemical shifts values and coupling constants in the ^{31}P NMR spectra of these molecules, compared to their analogues

Chart I

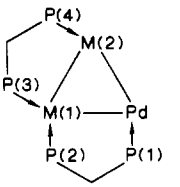

M(1) = Pd, Pt
M(2) = Mn, Fe

with Co or Fe. Steric effects can also be appreciated from the solid-state structure of **4a**, which shows severe deformations of the $Pd_2Mn_2P_4$ unit compared to the situation in the analogous $[Pd_2Co_2(CO)_7(\mu\text{-}dppm)_2]$ cluster.[2a]

Spectroscopic Characterization. The infrared spectra of the clusters containing platinum are generally very similar to those of the dipalladium analogues (Table I). The neutral triangular clusters **2** exhibit a strong and broad ν(CO) absorption around 1827 cm^{-1} and a weaker one around 1877 cm^{-1}, indicating (semi) bridging carbonyls ligands (cf. the corresponding values of 1868 and 1900 cm^{-1} for the related carbonyls in $[Pd_2CoI(\mu_3\text{-}CO)_2(CO)(\mu\text{-}dppm)_2]$[2b]), and a very strong ν(NO) vibration around 1735 cm^{-1}. In compounds **3**, the stronger CO vibration is shifted by ca. 30 cm^{-1} to higher wavenumbers, in accordance with the cationic nature of the clusters. The new band at ca. 2065 cm^{-1} clearly indicates the terminally bound CO. The tetranuclear clusters **1** exhibit the additional ν(CO) and ν(NO) bands due to the $Fe(CO)_3NO$ fragment ligated to the triangular core. The highest frequency absorption band of the tetranuclear clusters **4** (2028 cm^{-1}) is clearly assigned to the linear carbonyls of the exocyclic $Mn(CO)_5$ fragment (linearity also indicated by the X-ray structure determination of **4a**). The ^1H NMR data are collected in Table II. The pattern resulting from the two inequivalent methylene groups of the dppm ligands bridging the edges of the triangle is typical of these molecules, and the assignment is made by comparison with the cobalt-containing clusters previously discussed. The two methylenic protons of the dppm bridging the Pd (Pt)–metal bond always give rise to a triplet with a ^2J(PH) value in the range 8.5–10.5 Hz and, in the case of the platinum-containing clusters, to a further coupling of ca. 30–40 Hz with ^{195}Pt. The more downfield signal is attributed to the methylene of the other dppm and is more complicated. It generally appears as a doublet of triplet owing to coupling with the two P atoms of the ligand (^2J(PH) in the range 8–10 Hz) and to a further weak coupling (2–4 Hz) with a P atom of the neighboring dppm. A strong coupling with platinum (60–70 Hz) is evidenced for this CH_2 group in the platinum-containing clusters. Another effect resulting from the presence of platinum is a systematic downfield shift of both signals compared to those of the related dipalladium clusters. Changing the third metal of the triangle (Mn, Fe, or Co[2c]) affects only slightly the chemical shifts of both methylene groups, and the values in the Pd–Pd(Pt)–Fe clusters and their derivatives are very close to those found for the corresponding Pd–Pd(Pt)–Co clusters. The fact that replacing the exocyclic metalloligand $Fe(CO)_3NO$ with iodide has little effect on the methylene chemical shifts contrasts with the replacement with chloride, which causes a significant upfield shift of the CH_2 protons of the dppm bridging the Pd–Pd bond. On the other hand, going from neutral to cationic clusters of type **3a**, the chemical shifts of the methylene protons of each dppm are strongly increased. The $^{31}P\{^1H\}$ NMR data are given in Table III. The four phosphorus atoms of the dppm ligands are chemically inequivalent and are

(15) Pringle, P. G.; Shaw, B. L. *J. Chem. Soc., Dalton Trans.* **1983**, 889.

(16) (a) Hileman, J. C.; Huggins, D. K.; Kaesz, H. D. *Inorg. Chem.* **1962**, *1*, 933. (b) Knox, S. A. R.; Hoxmeier, R. J.; Kaesz, H. D. *Inorg. Chem.* **1971**, *10*, 2636. (c) Endrich, K.; Korswagen, R.; Zahn, T.; Ziegler, M. L. *Angew. Chem. Suppl.* **1982**, 1906.

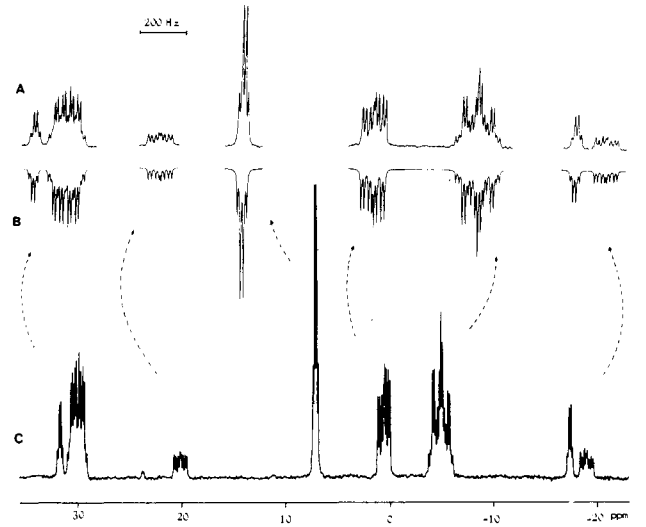

Figure 3. $^{31}P\{^1H\}$ NMR spectrum of $[PdPtFe(\mu\text{-}CO)_2(CO)(NO)(\mu\text{-}dppm)_2][PF_6]$ (**3b**): (A) expansion of the experimental spectrum; (B) calculated spectrum; (C) experimental spectrum. The phosphorus resonance of PF_6^- is not represented.

coupled to each other, giving rise to complex spectra (e.g., Figure 3). In most cases, the spectra have been fully analyzed and simulated by using the PANIC program (Bruker). The accuracy of the determination is ±5 Hz on the chemical shifts and ±0.5 Hz on the coupling constants. The assignment of the four phosphorus atoms, as it appears in Table III, follows from considerations previously detailed.[2c] Considering first the Fe-containing clusters, the chemical shift value of P(4) is found around 35 ppm, typical for a phosphorus bound to iron. Although the chemical shifts of P(1), P(2), and P(3) in the Pt-containing clusters are in the same range, P(2) and P(3) exhibit strong coupling constants with ^{195}Pt (3000–4000 Hz) which indicate that these nuclei are bound directly to platinum. Thus, P(1) can be unambigously assigned to the phosphorus atom bound to palladium. The assignment for the Pd_2Fe systems is made by comparison. The following general comments can be made: (i) J[P(1)P(2)] and J[P(1)P(4)] are the larger coupling constants and their values are roughly insensitive to the presence of palladium or platinum; (ii) J[P(1)P(3)] is always a small coupling constant although J[P(2)P(4)] which is also a three-bond "zigzag" coupling constant is higher; (iii) J[P(3)P(4)] is very small, and this could be explained by opposite signs of the ^2J and ^3J contributions leading to this coupling; (iv) J[P(2)P(3)] appears to be the only coupling constant strongly dependent on the nature of the metal Pd or Pt. It is small for phosphorus bonded to platinum in a cis position (6.5–14 Hz) but larger for phosphorus bonded to palladium (ca. 50 Hz). When the metalloligand $Fe(CO)_3NO$ in **1** is replaced by iodide, all the chemical shifts are found slightly upfield. The phosphorus most sensitive to a change of "exocyclic" ligand appears to be P(2). Its chemical shift variation is less pronounced when $Fe(CO)_3NO$ is replaced by CO in **3**. Note that in the latter clusters, all the coupling constants strongly decrease. The spectrum of the Pd_2Mn (**5a**) cluster exhibits four well-resolved and separated multiplets for each phosphorus atom and can be analyzed by using a first order approximation. The signal of the manganese-bound phosphorus P(4) (ca. 60 ppm) is slightly quadrupole broadened. As no equivalent spectrum exists for the complex with Pt in place of Pd, the attribution given in Table III is mainly based on the hypothesis that J[P(1)P(4)] is large. The strong downfield shift of P(2) compared to related molecules appears therefore to be the main feature of the spectrum.

Chart II

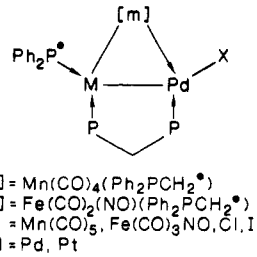

[m] = $Mn(CO)_4(Ph_2PCH_2^•)$
[m] = $Fe(CO)_2(NO)(Ph_2PCH_2^•)$
X = $Mn(CO)_5$, $Fe(CO)_3NO$, Cl, I
M = Pd, Pt

Bonding Description. A localized electron count about each metal of the 60-electron tetranuclear cluster **1** or **4** raises some difficulties with respect to the usual 18-electron or 16-electron configuration, respectively, about the Fe or Mn and the Pd or Pt centers, respectively. This is due, in part, to the semibridging nature of carbonyl ligands, which may result from both steric and electronic requirements. Similar problems are encountered with the 44-electron trinuclear clusters described in this work, although these total electron counts are consistent with tetranuclear, respectively trinuclear clusters, containing two metals which utilize eight valence orbitals only. However, a pleasing way of accounting for the remarkable bonding mode of the fragment $\mu\text{-}Mn(CO)_4(PPh_2R)$ (R = $CH_2^•$) in **4a** is to view it as globaly bridging the M–Pd (M = Pd, Pt) dinuclear unit. Thus, the anionic group $\mu\text{-}[Mn(CO)_4(PPh_2R)]^-$ behaves, like $\mu\text{-}[PPh_2]^-$ would, as a 4-electron donor toward the cationic 26-electron $[MPd(\mu\text{-dppm})(PPh_2^•)X]^+$ (X = Cl, I, $Fe(CO)_3NO$, $Mn(CO)_5$) unit, which contains two d^9 metal centers. Similar considerations applied to the 18-electron anionic $\mu\text{-}[Fe(CO)_2(NO)(PPh_2R)]^-$ fragment allow us to rationalize the bonding situation in the tri- and tetranuclear clusters described in this work (Chart II). These clusters therefore constitute novel examples where an anionic 18-electron metal carbonyl fragment is involved in a closo cluster structure.[3a,b,17]

Experimental Section

All reactions were performed under a prepurified N_2 atmosphere in Schlenk-type flasks. Solvents were distilled as previously described.[3] Reagents were used as received without further purification. Unless otherwise stated, the spectroscopic instruments employed in this research have been described previously.[2,3] Proton and carbon chemical shifts are positive downfield relative to external Me_4Si. $^{31}P\{^1H\}$ NMR spectra are externally referenced to 85% H_3PO_4 in H_2O, with downfield chemical shifts reported as positive. The ligand $Ph_2PCH_2PPh_2$ (dppm)[18] and the complexes $[Pd_2Cl_2(\mu\text{-dppm})_2]$[5] and $[PdPtCl_2(\mu\text{-dppm})_2]\cdot CH_2Cl_2$[15] were obtained by literature methods. Solutions of $Na[Mn(CO)_5]$ were prepared by Na/Hg reduction of a THF solution of $[Mn_2(CO)_{10}]$,[19] and $K[Fe(CO)_3NO]$ was prepared by the reaction of $[Fe(CO)_5]$ with KNO_2.[20]

$[Pd_2Fe_2(CO)_5(NO)_2(\mu\text{-dppm})_2]$ (1a). A solution of $K[Fe(CO)_3NO]$ (0.443 g, 2.12 mmol) in THF (50 mL) was added to a cooled (–78 °C) and stirred suspension of $[Pd_2Cl_2(\mu\text{-dppm})_2]$ (1.120 g, 1.06 mmol) in THF (50 mL). The mixture was protected from light by an aluminum foil wrapped around the flask. The reaction temperature was progressively raised to 0 °C (2 h) by replacing the acetone/dry ice bath with ice. The color of the mixture slowly turned from orange to deep violet. The temperature was then raised to 20 °C, and the color of the reaction mixture further

(17) (a) Bender, R.; Braunstein, P.; Metz, B.; Lemoine, P. *Organometallics* **1984**, *3*, 381. (b) Hofmann, P.; Schmidt, H. R. *Angew. Chem., Int. Ed. Engl.* **1986**, *25*, 837.
(18) Sommer, K. *Z. Anorg. Chem.* **1970**, *376*, 37.
(19) Gorsich, R. D. *J. Am. Chem. Soc.* **1962**, *84*, 2486.
(20) Hieber, W.; Beutner, H. *Z. Naturforsch., B: Anorg. Chem., Org. Chem., Biochem., Biophys., Biol.* **1960**, *B15*, 323.

changed to dark blue and then to deep green (8 h). The mixture was filtered on a class 4 glass frit to remove insoluble KCl and $[Pd_2Cl_2(\mu\text{-}CO)(\mu\text{-}dppm)_2]$ (0.36 g, 31% based on Pd, identified by comparison with an authentic sample[5]). Addition of *n*-hexane gave, after cooling at −20 °C, black-green microcrystals of **1a**. They were collected by filtration, washed with water to remove residual ionic species, dried in vacuo, and recrystallized from CH_2Cl_2/*n*-hexane (0.905 g, 66% based on Pd; mp 178 °C dec). Anal. Calcd for $C_{55}H_{44}Fe_2N_2O_7P_4Pd_2$ (M_r 1293.40): C, 51.08; H, 3.43; N, 2.17; P, 9.58; Fe, 8.66; Pd, 16.46. Found: C, 50.81; H, 3.75; N, 1.92; P, 9.27; Fe, 8.22; Pd, 15.35. The remaining brown-green mother liquor was evaporated to dryness. The extraction of the solid residue with pentane afforded ca. 0.050 g of a mixture of the yellow compounds $[\{Fe(CO)_4\}_2(\mu\text{-dppm})]$ (IR (pentane) ν(CO) 2051 (m), 1983 (m), 1950 (s), 1933 (s) cm^{-1})[6a] and $[\{Fe(CO)(NO)_2\}_2(\mu\text{-dppm})]$ (IR (pentane) ν(CO) 2013 (m), ν(NO) 1765 (s), 1726 (s) cm^{-1}).[6b]

$[PdPtFe_2(CO)_5(NO)_2(\mu\text{-dppm})_2]$ (1b). A solution of K[Fe(CO)$_3$NO] (1.03 g, 4.90 mmol) in THF (50 mL) was added to a cooled (0 °C) and stirred orange suspension of $[PdPtCl_2(\mu\text{-dppm})_2]\cdot CH_2Cl_2$ (2.82 g, 2.30 mmol) in THF (80 mL). The solution turned deep blue-green when the temperature was raised to ambient. After being stirred for 2.5 h, the solution was concentrated (to ca. 80 mL) in vacuo and filtered on a class 4 glass frit to remove KCl (0.33 g, 4.43 mmol, 90% based on K). Addition of pentane (120 mL) gave, after cooling at −20 °C, a dark green powder which was filtered off. Recrystallization of this powder in toluene (200 mL)/pentane (200 mL) gave, after cooling at −20 °C, dark blue-green microcrystalline **1b** (2.60 g, 1.88 mmol, 82% based on Pt). Anal. Calcd for $C_{55}H_{44}Fe_2N_2O_7P_4PdPt$ (M_r 1382.06): C, 47.80; H, 3.21; N, 2.03. Found: C, 48.01; H, 3.98; N, 1.78.

$[Pd_2Mn_2(CO)_9(\mu\text{-dppm})_2]$ (4a). A filtered solution of Na[Mn(CO)$_5$] in THF (0.20 M, 45.3 mL) was added to a cooled (−78 °C) and stirred suspension of $[Pd_2Cl_2(\mu\text{-dppm})_2]$ (4.770 g, 4.53 mmol) in THF (75 mL). No reaction occurred until the temperature was raised to 0 °C by replacing the acetone/dry-ice bath with ice. The color of the reaction mixture slowly changed from orange to brown-violet. After 4 h, the mixture was filtered on a class 4 glass frit to remove insoluble $[Pd_2Cl_2(\mu\text{-CO})(\mu\text{-dppm})_2]$ (0.712 g, 14.5% based on Pd, characterized by ^1H and $^{31}P\{^1H\}$NMR and IR spectroscopy[5]) and NaCl (eliminated with water). The volume of the filtrate was reduced to ca. 50 mL by evaporation under vacuum. Pentane (150 mL) was added to the solution which was cooled to −20 °C to induce precipitation. The resulting brown powder was collected by filtration (at 0 °C, as for all subsequent workup). This crude solid was partially dissolved in THF until the color of the resulting solution had become faint violet. THF was then replaced by *freshly distilled* CH_2Cl_2 which extracted cluster **4a** as a deep violet solution. Addition of *n*-hexane to this solution afforded, after cooling at −20 °C, a violet microcrystalline powder of **4a** (1.537 g, 25.3% based on Pd). The brown filtrate, combined with the THF extract, was evaporated to dryness, and the residue was chromatographed on a Celite column. Elution with pentane produced a yellow solution of $[Mn_2(CO)_{10}]$ (0.31 g, 17.5% based on Mn, characterized by IR spectroscopy), pentane/toluene (4:1) gave a yellow solution of $[Mn_2(CO)_8(\mu\text{-dppm})]$ (0.17 g, 5% based on Mn, characterized by IR (THF) ν(CO) 2056 (s), 2009 (m), 1991 (s), 1969 (vs), 1917 (m) cm^{-1}),[9] and further elution with toluene gave a red solution of **6a** (0.95 g, 10% based on Pd, after recrystallization from *n*-hexane). Elution with THF gave a brown solution of an unidentified compound X (0.75 g after recrystallization from *n*-hexane).

4a: mp 170–174 °C dec; $^{31}P\{^1H\}$ NMR (toluene/toluene-d_8) δ 72.6 (1 P, quadrupole broadened, J(PP) ≈ 86 Hz, P→Mn), 15.7–9.3 (3 P, unresolved m, P→Pd). Anal. Calcd for $C_{59}H_{44}Mn_2O_9P_4Pd_2$ (M_r 1343.61): C, 52.74; H, 3.30; P, 9.22. Found: C, 53.03; H, 3.62; P, 9.04.

6a: mp 216 °C dec; IR (KBr) ν(CO) 1917 (m), 1850 (s), 1815 (m) cm^{-1}; IR (THF) ν(CO) 1930 (m), 1864 (s) cm^{-1}; far-IR (polyethylene disk) ν(PdCl) 267 (m) cm^{-1}; ^1H NMR (CD_2Cl_2) δ 7.79–7.20 (40 H, m, Ph), 3.86 (4 H, quint, $|^2J(PH) + {}^4J(PH)|$ = 5 Hz, CH_2); $^{31}P\{^1H\}$ NMR (CD_2Cl_2, recorded at 36 MHz) δ 77.0 (2 P, t) 23.7 (2 P, t), apparent value of J(PP) in the AA′XX′ spectrum = 59 Hz; $^{13}C\{^1H\}$ NMR ($CDCl_3$) δ 236 (t, $^2J(PC)$ = 18.7 Hz, CO), 227 (t, $^2J(PC)$ = 33 Hz, CO), 137–126 (m, Ph), 44 (CH_2). Anal. Calcd for $C_{53}H_{44}ClMnO_3P_4Pd$ (M_r 1049.64): C, 60.65; H, 4.23; Cl, 3.38; Mn, 5.23; P, 11.80; Pd, 10.14. Found: C, 60.19; H, 4.31; Cl, 3.38; Mn, 5.39; P, 9.62; Pd, 10.48.

Compound X: IR (KBr) ν(CO) 2022 (s), 1906 (vs, br) cm^{-1}; ^1H NMR ($CDCl_3$) δ 7.80–6.74 (20 H, m, Ph), 3.73 (2 H, br m, CH_2); decomposed on MS runs. Anal. Found: C, 42.25; H, 3.33; P, 8.04; Pd, 19.38; Mn, 7.75.

Decomposition of 4a in Solution. A violet solution of **4a** (ca. 0.025 g, 0.02 mmol) in THF (5 mL) was stirred for 3 h at room temperature. The solution slowly turned red-brown. The solvent was removed under vacuum, and the solid residue was washed with *n*-hexane which colored pale yellow. The IR spectrum of the residue showed the characteristic CO absorption bands of X (see above).

Reaction of $[PdPtCl_2(\mu\text{-dppm})_2]$ with Na[Mn(CO)$_5$]. A solution of Na[Mn(CO)$_5$] (0.05 M) in THF (70 mL) was added to a cooled (−78 °C) and stirred orange suspension of $[PdPtCl_2(\mu\text{-dppm})_2]\cdot CH_2Cl_2$ (1.85 g, 1.62 mmol) in THF (100 mL). The solution turned green-brown when the temperature was raised to ambient. After being stirred for 2 h, the solution was concentrated (to ca. 100 mL) in vacuo and the product precipitated with *n*-hexane. The dark green-brown solid was filtered off and washed with water (600 mL). Extraction with toluene (50 mL)/*n*-hexane (150 mL) gave an orange-red solution, containing, i.e., $[Mn_2(CO)_{10}]$ (identified by IR), and a green solid identified as **4b** (0.400 g, 17% based on Pt), by comparison of its IR spectroscopic data with those of **4a**. All attempts to purify **4b**, by, e.g., crystallization from THF (40 mL)/*n*-hexane (40 mL), failed and led to partial transformation of **4b** into the cationic bimetallic complex $[(CO)_4Mn(\mu\text{-dppm})Pt(dppm)]^+$ (**7b**), identified by $^{31}P\{^1H\}$ NMR spectroscopy.[12]

$[Pd_2FeI(CO)_2(NO)(\mu\text{-dppm})_2]$ (2a). A solution of KI (2.55 g, 20-fold excess) in acetone/(25 mL)/water (5 mL) was added to a solution of **1a** (1.01 g, 0.780 mmol) in acetone (50 mL). The resulting red-brown solution was stirred for 1 h (note that complete evaporation of the solvents at this stage leads to the reformation of green **1a** and that numerous solubilization–evaporation cycles could be performed without decomposition). Addition of *n*-hexane (200 mL) induced precipitation of a solid that was recovered by filtration and vacuum dried. The yellow filtrate was evaporated to dryness, and an IR (THF) spectrum of this residue showed the presence of $[Fe(CO)_3NO]^-$. The red-brown solid was dissolved in toluene (300 mL), and the resulting solution was filtered and concentrated to ca. 100 mL by evaporation. Addition of *n*-hexane (100 mL) afforded analytically pure **2a** as red-brown microcrystals (0.925 g, 95% based on Pd). Anal. Calcd for $C_{52}H_{44}FeINO_3P_4Pd_2$ (M_r 1250.42): C, 49.95; H, 3.55; N, 1.12. Found: C, 49.98; H, 3.65; N, 1.03.

$[PdPtFeI(CO)_2(NO)(\mu\text{-dppm})_2]$ (2b). Solid KI (0.580 g, 3.50 mmol) was added to a stirred solution of **1b** (0.970 g, 0.702 mmol) in acetone (100 mL). The dark green solution immediately turned red. After the mixture was stirred for 1 h, the solvent was evaporated in vacuo. The red solid residue was washed with water (500 mL) to remove K[Fe(CO)$_3$NO] (identified by its IR absorptions in THF at 1990 (s), 1976 (m), 1886 (vs), 1848 (m), 1650 (s), and 1616 (s) cm^{-1}; 0.135 g, 46% based on Fe) and excess KI. Extraction with Et_2O (200 mL) gave a green solution of **1b**. Further extraction with CH_2Cl_2 (50 mL) afforded a red solution of **2b**. Addition of *n*-hexane (100 mL) at −20 °C gave a red powder of **2b** (0.816 g, 0.61 mmol, 87% based on Pt). Anal. Calcd for $C_{52}H_{44}FeINO_3P_4PdPt$ (M_r 1339.08): C, 46.64; H, 3.31; N, 1.05. Found: C, 46.54; H, 3.42; N, 0.93.

$[Pd_2MnCl(CO)_4(\mu\text{-dppm})_2]$ (5a). Method A. A solution of **4a** (0.430 g, 0.320 mmol) in nonfreshly distilled CH_2Cl_2 (50 mL) was stirred for ca. 8 h at room temperature. The solution slowly turned from violet to brown-green. The mixture was filtered, and a layer of *n*-hexane was added, giving a microcrystalline powder of **5a** (0.279 g, 66% based on Pd; mp 198 °C dec). Anal. Calcd for **5a**·1.5CH_2Cl_2 ($C_{55.5}H_{47}Cl_4MnO_4P_4Pd_2$) ($M_r$ 1311.47): C, 50.83; H, 3.61; P, 9.45; Pd, 16.23; Mn, 4.19. Found: C, 49.81; H, 3.75; P, 10.11; Pd, 16.78; Mn, 6.58. It is noteworthy that **5a** is pale green in solution, or in a finely divided powdery state in transmitted light, and violet in crystalline state in reflected light. After removal of solid **5a**, further precipitation of the mother liquor gave a light red-brown powder that was identified by IR spectroscopy as X (ca. 0.02 g) (see above).

Method B. Hydrochloric acid (ca. 0.1 N, 0.4 mL, prepared by dilution of HCl, 38% in degassed water) was added to a solution

of **4a** (0.021 g, 0.016 mmol) in freshly distilled CH_2Cl_2 (5 mL). The reaction mixture slowly turned from violet to green-brown. After 1 h, the solution was evaporated to dryness, and the residue was washed with water. An IR spectrum of the solid showed the bands of **5a** together with a band at 2015 (w) cm^{-1}. The residue was extracted with toluene, giving a green solution and leaving an insoluble brown material. The solution was filtered, and addition of *n*-hexane induced precipitation of **5a** (0.015 g, ca. 80% based on Pd).

Reaction of 4a with Chlorinated Solvents. A deep violet solution of **4a** (ca. 0.020 g, 0.015 mmol) in *freshly distilled* CH_2Cl_2 (5 mL) was stirred for 1.5 h at room temperature. No color change occurred. Few drops of commercial grade $CDCl_3$ were then added, and after 5 min the solution had turned green. The solvents were removed in vacuo, and the IR (KBr) spectrum of the residue showed the characteristic ν(CO) absorption bands of **5a**, together with bands at 2092 (vw) and 2015 (w) cm^{-1}, not assigned.

Reaction of 4a with Halides. 1. Reaction with $[NEt_4]Cl$. Solid $[NEt_4]Cl$ (0.060 g, 0.36 mmol, twofold excess) was added to a stirred suspension of freshly prepared **4a** (0.230 g, 0.171 mmol) in THF (20 mL). Upon stirring for 1.5 h, the mixture turned brown-green. The solvent was removed in vacuo, and the resulting crude solid was placed on a glass frit, washed with water (which colored in pale yellow) to remove salts, and dried. It was only partially soluble in THF, affording a brown-green filtrate. The insoluble material was solubilized with CH_2Cl_2, giving a violet solution of **4a** (unreacted or reformed?). Some brown insoluble material remained on the glass frit. *n*-Hexane was added to the THF brown-green solution, inducing the precipitation of a powder that was collected by filtration. An IR spectrum of the solid showed a mixture of **5a** and X. The presence of *fac*-$[MnCl(CO)_3(dppm)]$ in the mother liquor was identified by IR and ^1H NMR spectroscopy.[13]

2. Reaction with KI. The same procedure as above was applied to the reaction of **4a** with KI. A small amount of **4a** and decomposition products of **4a** (i.e., X) were recovered.

3. Reaction with [PPN]Cl. The mixture of **4a** and [PPN]Cl turned brown-green, and only X and *fac*-$[MnCl(CO)_3(dppm)]$ were recovered.

4. Solvent Effect on the Reaction of 4a with NaCl. When **4a** (0.020 g, 0.015 mmol) was treated with NaCl (large excess) in THF (2 mL), no reaction occurred, owing to the very low solubility of NaCl in this medium. Adding a few drops of water caused a slow browning of the solution. The same effect was observed when the reaction of **4a** with NaCl was carried out in CH_2Cl_2 instead of THF. By contrast, when the reaction was carried out in aqueous acetone, the mixture turned to the green color characteristic of **5a**. Adding immediately *n*-hexane to this solution caused the return to the original violet color of **4a** which re-formed.

Reaction of 1a or 2a with CO. Freshly prepared **1a** (0.080 g, 0.06 mmol) was dissolved in THF (20 mL) and stirred under CO at atmospheric pressure. After 18 h, **1a** was recovered unchanged. The same procedure was applied to **2a**, and no reaction occurred.

$[Pd_2Fe(CO)_3(NO)(\mu\text{-dppm})_2][PF_6]$ (3a). The following reaction and workup procedures were performed under a CO atmosphere. Solid $Tl[PF_6]$ (0.040 g, 0.114 mmol) was added to a solution of **2a** (0.136 g, 0.109 mmol) in CO-saturated acetone (30 mL). An immediate color change from red-brown to yellow-brown occurred, and formation of a precipitate of TlI was observed. Stirring and CO bubbling were maintained for 0.5 h. The solution was filtered on a Celite-padded filter funnel. Addition of *n*-hexane induced precipitation of a yellow-brown powder. Recrystallization in THF/*n*-hexane afforded pure **3a** (0.130 g, 92% based on Pd). Anal. Calcd for $C_{53}H_{44}F_6FeNO_4P_5Pd_2$ (M_r 1296.49): C, 49.10; H, 3.42; N, 1.08. Found: C, 48.94; H, 3.36; N, 0.98.

Reversible CO-Uptake Experiments. A solution of **3a** (0.050 g, 0.040 mmol) in THF (10 mL) was evaporated to dryness, causing a change of color from the starting yellow-brown solution to a green solid residue, insoluble in toluene. Dissolution in THF afforded an orange solution whose IR spectrum showed the diminution of the ν(CO) vibration at 2069 cm^{-1}. Bubbling CO into this solution immediately caused the lightening of the solution and the complete restoration of the ν(CO) vibration band at 2069 cm^{-1}. The same observations were made when acetone, methanol, or CH_2Cl_2 was used instead of THF as solvent.

Table V. Summary of Crystal Data and Intensity Collection Parameters for $[Pd_2Mn_2(\mu_3\text{-}CO)(\mu\text{-}CO)(CO)_7(\mu\text{-}Ph_2PCH_2PPh_2)_2]\cdot C_6H_5Cl$ ($4a\cdot C_6H_5Cl$)

formula	$C_{65}H_{49}ClMn_2O_9P_4Pd_2$
fw	1456.13
cryst syst	monoclinic
space group	$P2_1/c$
cryst dimens, mm	0.28 × 0.28 × 0.36
cryst color and habit	violet prism
a, Å	17.561 (7)
b, Å	21.319 (8)
c, Å	19.461 (8)
β, deg	113.50 (2)
Z	4
V, Å^3	6681 (9)
ρ(calcd), g·cm^{-3}	1.44
ρ(obsd), g·cm^{-3}	1.42 ± 0.02
F(000), e	2920
temp, °C	20
diffractometer	Picker
radiation (graphite monochromator)	Mo Kα (λ(Mo Kα_1) = 0.710 73 Å)
linear abs coeff, cm^{-1}	10.62
transmissn factors: max, min	1.78, 1.47
scan mode	θ–2θ step–scan
scan width, deg	0.95 + 0.346 tan θ
step width, deg	0.04
scan speed, deg s^{-1}	0.016
2θ limits, deg	4–60
octants collcd	$h,k,\pm l$
no. of data collected	9611
no. of unique data used	4473, $I > 3\sigma(I)$
$R = \sum\|\|F_o\| - \|F_c\|\|/\sum\|F_o\|$	0.059
$R_w = [\sum w(\|F_o\| - \|F_c\|)^2/\sum w\|F_o\|^2]^{1/2}$	0.082
std error in an observn of unit weight, e	1.76
largest shift/esd, final cycle	0.07
largest peak in final diff map, e/Å^3	0.21

Reaction of 3a with NaCl. A solution of NaCl (tenfold excess) in aqueous acetone was added to a solution of **3a** (0.030 g, 0.023 mmol) in acetone (5 mL). The mixture turned to red-brown, and the solvents were evaporated to dryness. The residue was extracted with CH_2Cl_2 and filtered. Precipitation with *n*-hexane afforded a red-brown powder of a product spectroscopically identified as $[Pd_2FeCl(CO)_2(NO)(\mu\text{-dppm})_2]$.

$[PdPtFe(CO)_3(NO)(\mu\text{-dppm})_2][PF_6]$ (3b). The following reactions and manipulations were performed under a CO atmosphere. Carbon monoxide was bubbled for 0.5 h through a red mixture of **2b** (0.602 g, 0.45 mmol) and $Tl[PF_6]$ (0.168 g, 0.48 mmol) in THF (80 mL). An immediate color change to orange-red occurred, and a yellow precipitate of TlI formed. The solution was filtered through a Celite-padded filter funnel (medium porosity) and its volume reduced to ca. 40 mL. CO was bubbled through the solution again to ensure saturation, and addition of pentane (200 mL) afforded a red powder of **3b** (0.567 g, 0.41 mmol, 91% based on Pt). Anal. Calcd for $C_{53}H_{44}F_6FeNO_4P_5PdPt$ (M_r 1385.15): C, 45.96; H, 3.20; N, 1.01. Found: C, 44,46; H, 3.20; N, 0.95.

Reversible CO-Uptake Experiments. A solution of **3b** (0.057 g, 0.041 mmol) in THF (10 mL) was evaporated to dryness, causing a change of color from the starting orange-red solution to a red-brown solid. Dissolution in THF afforded an orange-brown solution whose IR spectrum showed new bands at 1847 (s, br) and at 1740 (vs) cm^{-1}, probably due to $[PdPtFe(CO)_2(NO)(THF)(\mu\text{-dppm})_2][PF_6]$, and a residual absorption at 2067 (w) cm^{-1}. Bubbling CO into this solution immediately restored the orange-red color and the intensity of the ν(CO) band at 2067 (vs) cm^{-1}.

Reaction of 3b with NaOCHO. Solid NaOCHO (0.006 g, 0.08 mmol) was added to a red solution of **3b** (0.097 g, 0.07 mmol) in acetone (20 mL). After being stirred for 0.5 h, the solution turned green, and 4 h later its color had changed to dark blue-green. $^{31}P\{^1H\}$ NMR data of the reaction mixture (acetone/acetone-d_6): δ 42.1 (m, 1 P, P→Fe), 9.3 (m, 1 P, P→Pt, ^1J(PtP) = 4375 Hz),

Table VI. Positional Parameters and Their Estimated Standard Deviations for 4a•C_6H_5Cl

atom	x	y	z	B, Å²	atom	x	y	z	B, Å²
Pd(1)	0.29184 (6)	0.08417 (4)	0.17519 (5)	3.98 (2)	C(35)	0.423 (1)	−0.3014 (7)	0.2128 (9)	7.8 (5)
Pd(2)	0.29502 (6)	−0.03703 (4)	0.13970 (5)	3.76 (2)	C(36)	0.448 (1)	−0.2458 (7)	0.2087 (9)	7.1 (5)
Mn(1)	0.3135 (1)	−0.00944 (8)	0.27453 (9)	4.01 (5)	C(37)	0.4001 (9)	−0.1960 (6)	0.1903 (8)	6.0 (4)
Mn(2)	0.2480 (1)	0.19994 (9)	0.2195 (1)	5.55 (6)	C(38)	0.1877 (7)	−0.1345 (5)	0.2095 (6)	4.3 (3)
P(1)	0.3057 (2)	0.1006 (1)	0.0627 (2)	3.97 (8)	C(39)	0.2939 (8)	−0.1441 (5)	0.3696 (6)	4.8 (3)
P(2)	0.3578 (2)	−0.0309 (1)	0.0530 (2)	4.09 (8)	C(40)	0.291 (1)	−0.2079 (7)	0.3630 (8)	7.3 (5)
P(3)	0.2481 (2)	−0.1344 (1)	0.1502 (2)	3.91 (8)	C(41)	0.334 (1)	−0.2446 (7)	0.427 (1)	9.0 (6)
P(4)	0.2369 (2)	−0.0887 (1)	0.2952 (2)	4.44 (9)	C(42)	0.3728 (9)	−0.2212 (7)	0.4916 (8)	6.6 (4)
C(1)	0.3379 (8)	0.1778 (5)	0.0440 (6)	4.8 (3)	C(43)	0.381 (1)	−0.1586 (8)	0.4996 (8)	10.7 (7)
C(2)	0.4208 (9)	0.1969 (6)	0.0864 (7)	5.9 (4)	C(44)	0.340 (1)	−0.1209 (6)	0.4387 (8)	7.8 (5)
C(3)	0.4430 (9)	0.2537 (7)	0.0740 (8)	6.5 (4)	C(45)	0.1496 (8)	−0.0727 (6)	0.3193 (6)	5.1 (3)
C(4)	0.3944 (9)	0.2933 (7)	0.0183 (8)	6.7 (4)	C(46)	0.0972 (9)	−0.1183 (6)	0.3249 (8)	6.8 (4)
C(5)	0.317 (1)	0.2789 (6)	−0.0205 (8)	7.5 (5)	C(47)	0.035 (1)	−0.1053 (9)	0.3463 (9)	9.6 (5)
C(6)	0.2838 (8)	0.2175 (6)	−0.0099 (7)	5.1 (4)	C(48)	0.021 (1)	−0.041 (1)	0.3631 (9)	9.1 (6)
C(7)	0.2146 (8)	0.0803 (5)	−0.0201 (6)	4.8 (3)	C(49)	0.0647 (9)	−0.0003 (8)	0.3523 (8)	8.2 (4)
C(8)	0.2150 (9)	0.0866 (6)	−0.0913 (7)	5.6 (4)	C(50)	0.129 (1)	−0.0098 (7)	0.3299 (8)	7.1 (4)
C(9)	0.144 (1)	0.0661 (7)	−0.1546 (8)	8.1 (5)	C(51)	0.2085 (8)	0.0112 (6)	0.1960 (6)	4.8 (3)
C(10)	0.076 (1)	0.0447 (8)	−0.144 (1)	9.6 (6)	O(1)	0.1386 (5)	0.0152 (4)	0.1582 (5)	5.2 (2)
C(11)	0.0790 (9)	0.0398 (6)	−0.0729 (7)	6.0 (4)	C(53)	0.3976 (9)	0.0399 (5)	0.2584 (6)	5.1 (3)
C(12)	0.1448 (8)	0.0549 (6)	−0.0122 (7)	4.9 (4)	O(3)	0.4617 (5)	0.0578 (4)	0.2667 (5)	6.2 (3)
C(13)	0.3868 (8)	0.0513 (5)	0.0533 (6)	4.2 (3)	C(52)	0.3272 (9)	0.0330 (6)	0.3586 (7)	5.8 (4)
C(14)	0.3144 (7)	−0.0520 (5)	−0.0451 (7)	4.1 (3)	O(2)	0.3340 (8)	0.0602 (5)	0.4106 (5)	9.2 (4)
C(15)	0.3511 (8)	−0.0362 (6)	−0.0954 (7)	5.7 (4)	C(54)	0.4036 (9)	−0.0634 (6)	0.3156 (7)	5.4 (4)
C(16)	0.315 (1)	−0.0486 (7)	−0.1689 (6)	7.0 (4)	O(4)	0.4592 (7)	−0.0917 (5)	0.3428 (6)	8.9 (4)
C(17)	0.242 (1)	−0.0822 (8)	−0.1938 (8)	7.6 (5)	C(59)	0.1825 (9)	0.1841 (7)	0.1251 (8)	6.4 (4)
C(18)	0.201 (1)	−0.0971 (7)	−0.1497 (8)	7.6 (5)	O(9)	0.1347 (8)	0.1835 (6)	0.0623 (7)	9.8 (4)
C(19)	0.2348 (8)	−0.0810 (6)	−0.0738 (7)	5.5 (4)	C(56)	0.3109 (9)	0.2527 (6)	0.1873 (7)	5.7 (4)
C(20)	0.4577 (8)	−0.0720 (5)	0.0896 (6)	4.4 (3)	O(6)	0.3443 (7)	0.2905 (5)	0.1704 (5)	8.0 (3)
C(21)	0.4757 (8)	−0.1206 (6)	0.0517 (6)	5.3 (3)	C(55)	0.1855 (9)	0.1512 (7)	0.2524 (9)	7.9 (5)
C(22)	0.551 (1)	−0.1522 (7)	0.0863 (9)	7.7 (5)	O(5)	0.1403 (7)	0.1262 (6)	0.2734 (7)	12.2 (4)
C(23)	0.6056 (9)	−0.1360 (7)	0.1553 (8)	6.8 (4)	C(57)	0.206 (1)	0.2649 (7)	0.2455 (9)	8.2 (5)
C(24)	0.5878 (9)	−0.0912 (6)	0.1972 (7)	5.8 (4)	O(7)	0.1757 (8)	0.3068 (6)	0.2610 (8)	11.5 (4)
C(25)	0.5160 (8)	−0.0594 (6)	0.1617 (7)	5.3 (3)	C(58)	0.3447 (9)	0.1798 (6)	0.2957 (7)	5.8 (4)
C(26)	0.1704 (8)	−0.1581 (5)	0.0592 (6)	5.1 (3)	O(8)	0.4072 (7)	0.1705 (5)	0.3466 (6)	8.2 (3)
C(27)	0.1023 (8)	−0.1184 (6)	0.0265 (7)	5.2 (4)	CS(1)	0.964 (2)	0.190 (1)	0.385 (2)	15 (1)
C(28)	0.045 (1)	−0.1331 (8)	−0.0437 (8)	7.4 (5)	CS(2)	0.991 (1)	0.236 (1)	0.421 (1)	12.6 (8)
C(29)	0.053 (1)	−0.180 (1)	−0.0826 (9)	10.4 (6)	CS(3)	1.020 (1)	0.278 (1)	0.394 (2)	15.5 (9)
C(30)	0.121 (1)	−0.2200 (8)	−0.0509 (8)	10.2 (6)	CS(4)	1.024 (1)	0.273 (1)	0.329 (1)	13.4 (8)
C(31)	0.178 (1)	−0.2086 (7)	0.0199 (8)	6.7 (4)	CS(5)	0.986 (3)	0.231 (2)	0.290 (2)	25 (2)
C(32)	0.3161 (8)	−0.1999 (5)	0.1812 (6)	4.3 (3)	CS(6)	0.965 (3)	0.183 (1)	0.311 (2)	25 (2)
C(33)	0.287 (1)	−0.2624 (6)	0.1847 (9)	7.4 (5)	ClS	0.9127 (8)	0.1270 (6)	0.417 (1)	29.2 (7)
C(34)	0.343 (1)	−0.3106 (6)	0.205 (1)	8.5 (5)					

[a] Anisotropically refined atoms are given in the form of the isotropic equivalent thermal parameters: B (Å²) = $(4/3)[\beta_{11}a^2 + \beta_{22}b^2 + \beta_{33}c^2 + \beta_{12}ab\cos\gamma + \beta_{13}ac\cos\beta + \beta_{23}bc\cos\alpha]$.

+8.5 to −0.5 (m, 2 P, P→Pd and P→Pt), −143.5 (hept, 1 P, PF_6, $^1J(PF)$ = 706 Hz).

Reaction of 5a with CO. CO was bubbled through a stirred solution of **5a** (0.060 g, 0.051 mmol) in THF (10 mL). Within 5 min, the color of the solution changed from green to red-brown. After CO bubbling was maintained for 0.5 h, the solvent was removed under vacuum. Extraction of the solid with *n*-hexane afforded a yellow solution of *fac*-[$MnCl(CO)_3$(dppm)], characterized as above. The IR spectrum of the hexane-insoluble brown residue showed a weak band at 1835 cm^{-1} in the ν(CO) region that later disappeared on further attempts of recrystallization.

X-ray Data Collection and Structure Determination of 4a•C_6H_5Cl. Single crystals of **4a**•C_6H_5Cl suitable for X-ray diffraction were obtained by slow diffusion of hexane into a PhCl solution of **4a** at −20 °C. A systematic search in reciprocal space using a Picker Facs-1 diffractometer showed that crystals of **4a** belong to the monoclinic system. The unit-cell dimensions and their standard deviations were obtained and refined at room temperature by using 25 carefully selected reflections and the standard Philips software. Final results are given in Table V. The single crystal was sealed in a Lindemann glass capillary and mounted on a rotation-free goniometer head. Table V gives the parameters used for data collection. The resulting data set was transferred to a PDP11/60 computer, and for all subsequent computations, the Enraf-Nonius SDP/V18 package was used,[21] with the exception of a local data reduction program. The standard reflections measured every hour during the entire data-collection period showed no significant trend in intensity. The raw step–scan data were converted to intensity by using the Lehmann and Larson method[22] and then corrected for Lorentz, polarization, and absorption factors, the latter computed by numerical integration method of Busing and Levy (transmission factor between 0.18 and 0.34).[23] The structure was solved by using the heavy-atom method. After refinement of the heavy atoms, a difference Fourier map revealed maxima of residual electronic density close to the positions expected for hydrogen atoms. They were introduced in structure factor calculations by their computed coordinates (C–H = 0.95 Å) and isotropic temperature factors of 7 Å², but not refined. Full least-squares refinement minimizing $\sum w(|F_o| - |F_c|)^2$ converged to the R values listed in Table V. Each reflection was weighted by using $\sigma^2(F) = \sigma^2_{counts} + (0.08I)^2$. A final difference map revealed no significant maxima. The scattering factor coefficients and anomalous dispersion coefficients are taken from ref 24. Final positional parameters are given in Table VI, and thermal parameters and observed and calculated structure factors are available as supplementary material.[25]

(21) Frenz, B. A. In *Computing in Crystallography*; Schenk, H., Olthof-Hazekamp, van Koningsveld, H., Bassi, G. S., Eds.; University Press: Delft, The Netherlands, 1978; p 64.

(22) Lehmann, M. S.; Larsen, F. K. *Acta Crystallogr., Sect. A: Cryst. Phys., Diffr., Theor. Gen. Crystallogr.* **1974**, *A30*, 580.

(23) Busing, W. R.; Levy, H. A. *Acta Crystallogr.* **1957**, *10*, 180.

(24) (a) Cromer, D. T.; Waber, J. T. *International Tables for X-Ray Crystallography*; Kynoch: Press: Birmingham, England, 1974; Vol. IV, Table 2-2b. (b) Cromer, D. T. *Ibid.* Table 2.3.1.

(25) See paragraph at the end of the paper regarding supplementary material.

Acknowledgment. We are grateful to the CNRS for financial support and for a grant to M.R. and to the Johnson Matthey Technology Center for a generous loan of $PdCl_2$.

Registry No. **1a**, 111026-19-8; **1b**, 111026-20-1; **2a**, 111026-21-2; **2b**, 111026-22-3; **3a**, 111026-26-7; **3b**, 111026-24-5; **4a**, 86028-11-7; **4a**·C_6H_5Cl, 111026-29-0; **4b**, 111026-28-9; **5a**, 111026-27-8; **6a**, 85688-54-6; **7b**, 111026-18-7; $\langle Fe(CO)(NO)_2\rangle_2(\mu$-dppm), 111026-17-6; $Pd_2FeCl(CO)_2(NO)(\mu$-dppm$)_2$, 111026-16-5; $[PdPtFe(CO)_2(NO)(THF)(\mu$-dppm$)_2][PF_6]$, 111059-92-8; $K[Fe(CO)_3NO]$, 25875-19-8; $Pd_2Cl_2(\mu$-dppm$)_2$, 64345-29-5; $Pd_2Cl_2(\mu$-CO$)(\mu$-dppm$_2)$, 64345-32-0; $\langle Fe(CO)_4\rangle_2(\mu$-dppm), 52843-17-1; $PdPtCl_2(\mu$-dppm$)_2$, 82307-36-6; $Na[Mn(CO)_5]$, 13859-41-1; $Mn_2(cO)_{10}$, 10170-69-1; $Mn_2(CO)_8(\mu$-dppm), 37523-60-7; *fac*-$[MnCl(CO)_3$(dppm)], 60305-98-8; $Tl[PF_6]$, 60969-19-9; Pd, 7440-05-3; Pt, 7440-06-4; Mn, 7439-96-5; Fe, 7439-89-6.

Supplementary Material Available: Tables of anisotropic thermal parameters (Table S-I), calculated hydrogen atom coordinates (Table S-II), complete bond lengths and angles (Tables S-III and S-IV), and selected weighted least-squares planes for **4a**·C_6H_5Cl (Table S-V) (9 pages); a listing of observed and calculated structure factors for **4a**·C_6H_5Cl (Table S-VI) (26 pages). Ordering information is given on any current masthead page.

Reactions of Transition-Metal σ-Acetylides. 11.[1] Cycloaddition Reactions with 1,1-Dicyano-2,2-bis(trifluoromethyl)ethene. X-ray Structures of $W\{\overline{C{=}CPhC(CF_3)_2C(CN)_2}\}(CO)_3(\eta\text{-}C_5H_5)$, $Mn\{\overline{C{=}CPhC(CF_3)_2C(CN)_2}\}(CO)_3$(dppe), and $Fe\{\overline{C{=}CPhC(CF_3)_2C(CN)_2}\}(CO)_2(\eta\text{-}C_5H_5)$ and of a Hydration Product, $\overline{W\{NH{=}C(OH)C(CN){=}CCPh{=}C(CF_3)_2\}}(CO)_2(\eta\text{-}C_5H_5)\cdot H_2O$

Michael I. Bruce,* Michael J. Liddell, Michael R. Snow, and Edward R. T. Tiekink

Jordan Laboratories, Department of Physical and Inorganic Chemistry, University of Adelaide, Adelaide, South Australia 5001

Received May 22, 1987

Reactions between $W(C_2Ph)(CO)_3(\eta\text{-}C_5H_5)$ (**6**), $Mn(C_2Ph)(CO)_3$(dppe) (**7**), or $Fe(C_2Ph)(CO)_2(\eta\text{-}C_5H_5)$ (**8**) and $(CF_3)_2C{=}C(CN)_2$ give the corresponding σ-cyclobutenyl complexes, all of which have been fully characterized by X-ray crystallography. The butadienyl complex $Ni\{C[{=}C(CN)_2]CPh{=}C(CF_3)_2\}(PPh_3)(\eta\text{-}C_5H_5)$ (**11**) was obtained from $Ni(C_2Ph)(PPh_3)(\eta\text{-}C_5H_5)$ and the cyanofluoro olefin. Heating **6** in refluxing xylene resulted in ring opening to give $W\{C[{=}C(CN)_2]CPh{=}C(CF_3)_2\}(CO)_3(\eta\text{-}C_5H_5)$ (**9**) and the related allyl complex $W\{\eta^3\text{-}C(CF_3)_2CPhC{=}C(CN)_2\}(CO)_2(\eta\text{-}C_5H_5)$ (**10**). Attempts to prepare **10** by reaction of **6** with Me_3NO gave instead $\overline{W\{NH{=}C(OH)C(CN){=}CCPh{=}C(CF_3)_2\}}(CO)_2(\eta\text{-}C_5H_5)$ (**12**), confirmed by an X-ray study and formed by addition of H_2O to one of the CN groups, followed by chelation. Crystal data for **6**: monoclinic, space group Pn, a = 9.575 (2) Å, b = 7.493 (2) Å, c = 15.670 (4) Å, β = 103.79 (2)°, Z = 2; 2641 data were refined to R = 0.075, R_w = 0.079. Crystal data for **7**: orthorhombic, space group $P2_12_12_1$, a = 11.251 (2) Å, b = 17.888 (3) Å, c = 19.894 (3) Å, Z = 4; 2947 data were refined to R = 0.047, R_w = 0.050. Crystal data for **8**: monoclinic, space group $P2_1/a$, a = 11.430 (3) Å, b = 15.201 (3) Å, c = 11.887 (2) Å, β = 102.50 (2)°, Z = 4; 2756 data were refined to R = 0.044. Crystal data for **12**: monoclinic, space group $C2/c$, a = 16.089 (3) Å, b = 10.003 (2) Å, c = 32.569 (5) Å, β = 104.2 (1)°, Z = 8; 2433 data were refined to R = 0.042, R_w = 0.047.

Introduction

A detailed study of the reactions between several transition-metal σ-acetylides and tetracyanoethene [tcne, $C_2(CN)_4$] (Scheme I) has shown that cyclobutenyl (**1**), buta-1,3-dien-2-yl (**2**), and allylic (**3**) complexes are formed from an initial, as yet uncharacterized paramagnetic adduct.[2,3] Some related complexes have been obtained from substituted styrenes $4\text{-}RC_6H_4CH{=}C(CN)(R')$ (R = NO_2 or H; R′ = CN or CO_2Et), one of which was characterized by an X-ray study as **4**. The observed direction of addition of the olefin suggests the intermediacy of a relatively stable dicyanomethide anion, perhaps in a zwitterionic complex such as **5**.[4]

Scheme I. Cycloaddition and Subsequent Reactions of $C_2(CN)_4$ with Transition-Metal Acetylides

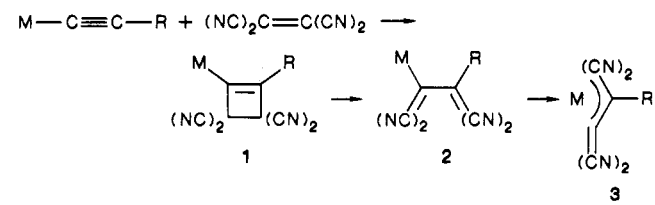

This paper describes some of our studies of the related olefin 1,1-dicyano-2,2-bis(trifluoromethyl)ethene [C-

(1) For part 10 see: Bruce, M. I.; Duffy, D. N.; Liddell, M. J.; Snow, M. R.; Tiekink, E. R. T. *J. Organomet. Chem.*, in press.
(2) Bruce, M. I.; Hambley, T. W.; Snow, M. R.; Swincer, A. G. *Organometallics* **1985**, *4*, 494.
(3) Bruce, M. I.; Hambley, T. W.; Snow, M. R.; Swincer, A. G. *Organometallics* **1985**, *4*, 501.
(4) Bruce, M. I.; Humphrey, P. A.; Snow, M. R.; Tiekink, E. R. T. *J. Organomet. Chem.* **1986**, *303*, 417.

0276-7333/88/2307-0343$01.50/0